10 B

PNL-3869
UC-21

Development of Damage Resistant Sputtered Oxide Optical Coatings for Use at 248 NM

W. T. Pawlewicz
P. M. Martin
D. D. Hays
I. B. Mann

October 1981

Prepared for
the Lawrence Livermore National Laboratory
under a Related Services Agreement
with the U.S. Department of Energy
Contract DE-ACO6-76RLO 1830

Pacific Northwest Laboratory
Operated for the U.S. Department of Energy
by Battelle Memorial Institute

Battelle

PNL-3869

PACIFIC NORTHWEST LABORATORY
operated by
BATTELLE
for the
UNITED STATES DEPARTMENT OF ENERGY
Under Contract DE-AC06-76RLO 1830

Printed in the United States of America
Available from
National Technical Information Service
United States Department of Commerce
5285 Port Royal Road
Springfield, Virginia 22151

Price: Printed Copy $_____*; Microfiche $3.00

*Pages	NTIS Selling Price
001-025	$4.00
026-050	$4.50
051-075	$5.25
076-100	$6.00
101-125	$6.50
126-150	$7.25
151-175	$8.00
176-200	$9.00
201-225	$9.25
226-250	$9.50
251-275	$10.75
276-300	$11.00

PNL-3869
UC-21

DEVELOPMENT OF DAMAGE RESISTANT SPUTTERED OXIDE OPTICAL COATINGS FOR USE AT 248 NM

W.T. Pawlewicz
P.M. Martin
D.D. Hays
I.B. Mann

October 1981

Prepared for
the Lawrence Livermore National Laboratory
under a Related Services Agreement with the
U.S. Department of Energy Contract DE-AC06-76RLO 1830

Pacific Northwest Laboratory
Richland, Washington 99352

SUMMARY

This report summarizes the results of a six-month effort to develop damage-resistant Kr*F laser mirrors by using and refining reactive sputter deposition techniques for the fabrication of multilayer oxide optical coatings. Mirror performance goals included a reflectivity of 99% at 248 nm and a laser damage threshold of 5 J/cm^2 for 20 ns pulses. Above and beyond these goals, however, particular attention was to be paid to improvement of the physical and optical properties of the coatings with the goal of extending to shorter wavelengths the ultraviolet absorption edge of candidate multilayer combinations.

Oxide multilayer coating combinations selected for development were SiO_2/Al_2O_3, SiO_2/HfO_2 and SiO_2/Y_2O_3. Selection was based on review and compilation of the optical properties of oxide materials reported in the recent literature. Twenty-eight coatings of selected designs were fabricated on LLNL substrates for laser damage testing by LLNL. Forty other coatings were fabricated on PNL substrates for optical, microstructural and topographical characterization by PNL aimed at optimization of their performance. Specimens for damage testing consisted of single layers of Al_2O_3, HfO_2 and Y_2O_3 in thicknesses of $\lambda/2$, $3\lambda/2$ and 2λ at 248 nm plus high reflectors of the design LL $(HL)^m$ HLL. In this design each layer is $\lambda/4$ at 248 nm, L is always SiO_2, and m = 19, 10 and 6 when H is Al_2O_3, Y_2O_3 and HfO_2, respectively.

Highest reflectivities at 248 nm were obtained for the HfO_2/SiO_2 combination for which the multipoint average of readings taken across the face of the 2-inch substrates was 94-96%. Reflectivities in excess of 99% were obtained in some regions of some of these mirrors. Average reflectivities for Al_2O_3/SiO_2 and Y_2O_3/SiO_2 were 80-83% and 62-80%, respectively.

Highest damage thresholds were obtained for Al_2O_3/SiO_2 and were always between 2.0 and 2.3 J/cm^2 for 20 ns pulses. For HfO_2/SiO_2 thresholds ranged from 0.9 to 2.1 J/cm^2, and for Y_2O_3/SiO_2 from 0.4 to 0.7 J/cm^2. Thus there was no obvious correlation between damage threshold and the reflectivity. The thresholds of the multilayer mirrors were also found to be very similar to those for single layer coatings. These were 1.5 to 3.2 J/cm^2 for Al_2O_3, 0.3 to 0.8 for HfO_2, and 0.3 to 1.1 for Y_2O_3. No evidence was found for two-photon damage processes from the threshold variation with absorption edge for these three coating materials. Damage resistance did not appear to depend on: (1) single-layer thickness, (2) stack tuned wavelength, (3) laser beam polarization, (4) substrate polishing technique, or (5) substrate cleaning technique. It did appear, however, that significant improvement in damage resistance could come from increased attention to coating cleanliness.

The low mirror reflectivities are due primarily to scattering by columnar surface features caused by insufficient control of the coating grain size. The damage thresholds for both single layers and multilayers may also be governed by the coating surface roughness. Scattering contributed by substrate roughness did not appear to be small. Thus the levels of stoichiometry and purity achieved appear to be adequate, and absorption due to intrinsic interband mechanisms does not appear to be important for any of these materials at 248 nm.

Although these results are short of the 99% and 5 J/cm^2 reflectivity and damage threshold goals of this work, optimization of the deposition of these coating materials to reduce surface roughness and scattering promises to yield improved performance.

Specific recommendations for minimizing coating surface roughness and for correcting other shortcomings of this mirror fabrication effort have been developed to guide future research.

CONTENTS

FIGURES

TABLES

INTRODUCTION

The objective of this work was the development of damage-resistant all-dielectric high reflectors for Kr*F lasers through the use and refinement of reactive sputter deposition techniques for the fabrication of multilayer oxide optical coatings. Specific performance goals included a reflectivity of 99% at 248 nm and a damage threshold of 5 J/cm^2 for 20 ns pulses. Particular attention was also to be paid to determination of coating physical properties or characteristics which limit their optical performance at ultraviolet wavelengths and to extension of the ultraviolet absorption edge to shorter wavelengths.

The work was carried out in three phases: (1) review and compilation of the recent literature for optical and physical properties of oxides leading to selection of HfO_2, Al_2O_3, Y_2O_3 and SiO_2 as the most promising candidates, (2) deposition of single layer coatings of HfO_2, Al_2O_3 and Y_2O_3 in integer multiples of half-wave thickness and (3) fabrication of multilayer high reflectors from combinations of HfO_2/SiO_2, Al_2O_3/SiO_2 and Y_2O_3/SiO_2. All coatings for damage testing were prepared on fused silica or Bk-7 glass substrates provided by LLNL and were shipped to LLNL. The coatings shipped and many others made on PNL substrates were characterized for optical, microstructural and topographical features with the intent of understanding the ultimate performance of each coating material in a high reflector stack and optimizing the performance of those stacks. However, it was recognized early on that limited time and funding would allow only a cursory optimization of each coating material and the multilayer reflectors made from them, and that a more detailed examination might be necessary as a follow-on effort.

This report summarizes all work conducted to date on sputtered oxides for use at the Kr*F wavelength. The Experimental section describes the deposition of single and multilayer oxide optical coatings by reactive sputtering and characterization of their optical and microstructual properties. Deposition and characterization are described in sufficient detail that the work could be repeated elsewhere and so that this report can serve as a starting point for a follow-on effort, should one be desired. Coating designs selected for damage testing are also described. The Results section summarizes in graphs and tables the most important optical property, structural property, and reflectivity data accumulated to date and all laser damage testing data received from LLNL. The Discussion section explains the ultraviolet optical properties of the coatings and the observed performance of the high reflector stacks. The Conclusion section summarizes all key results and is followed by Recommendations for Further Study. Finally, the complete compilation of optical and physical data accumulated in the literature survey of ultraviolet-transmitting oxide materials is included in this report as an Appendix.

EXPERIMENT

Sputtering System

All coatings were deposited in rf diode sputtering systems of the type shown schematically in Figure 1. The systems contained two water-cooled 6-inch diameter sputtering targets, a water-cooled substrate table which was rotated from one target to the next, and rotatable shutters for cleaning targets before deposition and for precise control of coating thickness. Substrate-target spacing was 1.5 inch. One target position was always occupied by the SiO_2 target. The second position was used for HfO_2, Al_2O_3 or Y_2O_3. Material, method of fabrication, vendor and purity of each target are summarized in Table 1. Each target was connected through an rf impedance matching network to an rf power supply operating at 13.56 MHz. Target power was typically 600 W. The matching network was always tuned for minimum reflected power.

Coatings were sputtered in atmospheres of Ar (99.9999% pure) and O_2 (99.9995% pure). Ar and O_2 were introduced to the system through flow meters and needle valves. Typical flows were 5 SCCM/min. Gases were mixed and the total pressure was measured with an absolute capacitance manometer. Typical sputtering pressure was 20 mTorr of which 15% was O_2, although some Al_2O_3 depositions were made with 50% O_2. The sputtering systems were mounted on conventional oil diffusion and mechanical pumps. A high-efficiency liquid nitrogen cold trap was used between the diffusion pump and the chamber to routinely attain pressures before deposition of 10^{-7} Torr. A variable orifice was used between the diffusion pump and the mechanical pump to throttle the flow of sputtering gases without reducing the H_2O pumping speed of the cold trap. The orifice conductance was ~ 20 l/s and the system throughput ~ 0.4 Torr l/s.

Substrate Preparation

Substrates were cleaned in two different ways. The first method, designated D in this report, involved simple scrubbing with liquid detergent and rinsing in deionized water. The second method, designated D+S, consisted of detergent scrubbing followed by cleaning with a high-pressure (3000 psi) spray of deionized water in commercially-available equipment.

Coating Designs

All single layers were made in thicknesses of $\lambda/2$, $3\lambda/2$ and 2λ, so that the coating/substrate transmission at 248 nm was that of the substrate minus any absorption and scattering. High reflectors were all of the design LL $(HL)^m$ HLL where each layer is $\lambda/4$, L is always SiO_2, and H is either Al_2O_3, Y_2O_3 or HfO_2. The number of coating pairs m for HfO_2 and Y_2O_3 was selected to yield a reflectivity of 99.9%, assuming no absorption or scattering losses. The number of coating pairs for Al_2O_3 was selected to yield a reflectivity of 99.2% to avoid very thick coatings which might scatter in the ultraviolet. For HfO_2, Y_2O_3 and Al_2O_3 m = 6, 10 and 19, respectively. A $\lambda/2$ SiO_2 overlayer and underlayer, designated LL above, were used with each high reflector but not with the single layers.

In some preliminary work not described elsewhere in this report, a 2:1 high reflector design of the form $(H'L')^mH'$, where $H' = \lambda/6$ and $L' = \lambda/3$ near 496 nm and m = 12, was tried for Y_2O_3/SiO_2 to simplify monitoring of layer thicknesses. However, the increased absorption and scattering associated with the thicker layers in this design caused lower reflectivities for the second-order peak at 248 nm that obtained with the first-order peak for the $\lambda/4$ stack described above.

Coating Deposition

Complete deposition conditions for each coating damage tested are listed in Table 2. Before each deposition was started, each target was sputter cleaned onto the rotatable shutter for 60 minutes under the same conditions used for deposition. This procedure removed any contamination from the target surface and also greatly reduced the residual pressure of H_2O, O_2 and N_2 in the chamber through the gettering action of the strongly reactive metals Si, Al, Hf and Y. Between layers of a stack, target power was momentarily reduced to zero, the substrate table was manually rotated to the next target, and target power was again increased to its desired value. Any tuning of the rf matching network required was done manually in the first 15 seconds of each layer deposition. Coating thickness was monitored by the product of target power and elapsed time. This procedure is quite adequate for sputtering, as opposed to evaporation,

because in sputtering the deposition rate is linearly proportional to the target power and reproducible to within a few percent from deposition to deposition.

Coating Characterization

All optical measurements were made with a double-beam, double-monochromator spectrophotometer operating for wavelengths of 200 to 2900 nm. Coating transmission accuracy is $\pm$ 0.2%. Reflectivity accuracy at 248 nm is $\pm$ 1%. Wavelength accuracy is $\pm$ 1 nm. The reflectivity of each mirror damage tested was measured at nine points arranged in an "x" pattern across the face of the substrate. A similar procedure was used for measurement of the tuned wavelength of a mirror.

Crystal structure, grain size and preferred orientation data were obtained using standard x-ray diffractometer techniques which involve analysis of peak location, peak strength and peak broadening. Diffractometer scans on thin optical coatings required long counting times and also digital data storage, manipulation and analysis. Data were collected at 0.05 degree intervals in the scattering angle 2 θ with 80s counting periods.

Coating surface topography was examined using Nomarski microscopy and SEM. Purity of selected coatings and all sputtering targets was verified by x-ray fluorescence examination, using x-ray excitation for targets and electron-beam excitation for coatings.

RESULTS

Laser Damage Thresholds

All laser damage data accumulated throughout this work are listed in Table 3 and plotted in Figure 2. In Table 3, coatings are identified by LLNL substrate number, LLNL damage testing number and PNL coating number, and are listed in the same order as in Table 2 which contains complete deposition condition information. Included for easy comparison with the damage threshold numbers are the coating material and design, any unusual deposition condition, tuned wavelength, mirror reflectivity, substrate material and polish, and the beam polarization for 10° incidence. Table 3 also contains comments made by LLNL damage testing personnel

concerning the overall appearance of the coatings and a ranking of their "cleanliness". Figure 2 plots damage threshold as a function of coating material and coating design, and also displays average thresholds for each design.

The highest damage thresholds were observed for Al_2O_3/SiO_2 with all four mirrors between 2.0 and 2.3 J/cm^2. One HfO_2/SiO_2 mirror damaged at 2.1 J/cm^2, but two others damaged at 1.0 and 0.9 J/cm^2. All five Y_2O_3/SiO_2 mirrors damaged between 0.4 and 0.7 J/cm^2.

In general the reflectors yielded damage thresholds comparable to the single-layer coatings of the same material. This result is most easily seen in Figure 2. Reflectors averaged 2.2 J/cm^2 for Al_2O_3/SiO_2, 1.3 J/cm^2 for HfO_2/SiO_2 and 0.6 J/cm^2 for Y_2O_3/SiO_2. Single-layer thresholds were 2.0, 0.6 and 0.6 J/cm^2, respectively. It may be important to note however that, inadvertently, all reflectors were deposited on Bk-7 glass and all single layers on fused silica. The damage thresholds do not increase in proportion to the optical band gaps or in inverse proportion to the refractive indices of these three materials, although highest thresholds were obtained for Al_2O_3 which does have the highest band gap and lowest refractive index.

No obvious correlation exists between damage thresholds and the reflectivities of the mirrors, as shown in Figure 3, although the results are not inconsistent with a correlation. Al_2O_3/SiO_2, with the highest thresholds, had intermediate reflectivities of 80-83%. HfO_2/SiO_2, with the highest reflectivities of 94-96%, had intermediate thresholds. For Y_2O_3/SiO_2, where reflectivities varied over a wide range from 67 to 80%, there also was no correlation with damage threshold.

No obvious correlation exists between damage threshold and tuned wavelength, as shown in Figure 4. This is particularly clear for Y_2O_3/SiO_2 mirrors for which tuned wavelengths range from 244 to 280 nm.

For the single-layer coatings, Al_2O_3 damaged at higher fluences when deposited with 50% O_2 in the sputtering gas than with 15% O_2. In fact, the two $\lambda/2$ Al_2O_3 coatings made with high O_2 partial pressure exhibited the highest thresholds of any single or multilayer coatings examined in this work. These thresholds were 2.6 and 3.2 J/cm^2. Higher O_2 partial pressure was therefore used for all subsequent multilayer depositions involving Al_2O_3.

There is no obvious correlation between the thickness of the single layers and their thresholds, as shown in Figure 5. For Al_2O_3, thresholds increase slightly with coating thickness for 15% O_2 coatings and decrease for 50% O_2. For HfO_2, thresholds increase or remain constant with increasing thickness. For Y_2O_3, thresholds decrease with increasing thickness.

Nearly identical results were obtained for Al_2O_3 single layers with the two substrate cleaning techniques D and D+S, for both O_2 partial pressures and for all three thicknesses involved. These results are also shown in Figure 5. Hence high-pressure water-spray cleaning does not appear to influence, and in particular does not decrease, damage thresholds as popularly believed. Note, however, that comparisons of the two cleaning techniques were made only for silica substrates and not Bk-7 glass.

No correlation is clearly apparent in Table 3 between damage threshold and substrate polishing technique, even though coatings were made and tested on (1) the front surface of conventionally polished substrates, (2) the rear surface of conventionally polished substrates, and (3) OCLI superpolished substrates.

No difference is obvious in Table 3 between results for p and s beam polarizations.

Finally, there does appear to be a correlation between damage threshold and the "cleanliness" ranking of the coatings. Here "cleanliness" is ranked from 0 (clean) to 3 (very dirty) by LLNL as a measure of the density of "submicron-sized artifacts" in the coatings. As shown in Figure 6, thresholds are grouped primarily by coating material rather than by cleanliness. But, within each coating material group, slightly higher thresholds are obtained for lower "cleanliness" rankings.

Mirror Reflectivities

Mirror reflectivities achieved with high reflector designs for the three coating materials combinations are displayed as a function of tuned wavelength in Figures 7, 8 and 9 for Al_2O_3/SiO_2, HfO_2/SiO_2 and Y_2O_3/SiO_2, respectively. Included in these figures are mirrors made on LLNL substrates for damage testing and mirrors made on PNL substrates for materials characterization. Coating identification numbers appearing in the figures are PNL coating numbers which

can be cross referenced to LLNL substrate or damage test numbers through the use of Table 2 or 3. For most coatings, nine points are plotted for measurements made in an "x" pattern across the face of the substrate. For some coatings, fewer measurements were made. The points thus plotted show two dependences: (1) the overall dependence of reflectivity on tuned wavelength for a particular pair of materials and (2) the variation of reflectivity across the face of individual coatings.

For Al_2O_3/SiO_2, reflectivities vary from as low as 74% to as high as 91% with a median value of 81%. The reflectivity is essentially independent of the tuned wavelength. For most individual coatings, the variation across the face of the substrate is $\pm$ 2% in reflectivity and $\pm$ 2% in tuned wavelength. Both variations are close to the precision limits of the spectrophotometer for wavelengths near 248 nm and thus may not be statistically significant.

For HfO_2/SiO_2, similar results are obtained except that the reflectivities are higher. Reflectivities range from 88 to 100% with a median value of 95%. The reflectivity is independent of wavelength for wavelengths greater than 220 nm, but for shorter wavelengths falls off rapidly. For most individual coatings, the variation across the face of the substrate is $\pm$ 2% in reflectivity and $\pm$ 1% in tuned wavelength. The spread in reflectivity values is largest for wavelengths less than 220 nm, as shown for coating #13I in Figure 8, and the reflectivity is lowest at the substrate center and highest at the perimeter.

For Y_2O_3/SiO_2, however, the results are quite different. Reflectivities as high as 85% are obtained for tuned wavelengths near 285 nm, but the reflectivity drops off rapidly for shorter wavelengths to 55% at 240 nm. Also note that, although the variation in tuned wavelength across the face of an individual coating is usually only $\pm$ 2%, the variation in reflectivity is typically $\pm$ 6% or larger. Finally, it is important to point out that the nine-point reflectivity profiling always showed highest reflectivity and longest tuned wavelength near the perimeter of the substrate, monotonically decreasing to the lowest reflectivity and shortest tuned wavelength near the substrate center.

The measured spectral dependence of the reflectivity is shown in Figures 10, 11 and 12 for some of the best Al_2O_3/SiO_2, HfO_2/SiO_2 and Y_2O_3/SiO_2 mirrors, respectively. Shown for comparison is the reflectivity spectrum for each coating combination calculated to include refractive index dispersion for each material. The large differences in the band width of the high reflectance region for the three combinations are due to differences in refractive index contrast or ratio. Taking into account the peak reflectance, the band width of the high reflectance region and the "squareness" of the high reflectance region, the HfO_2/SiO_2 combination is by far the best to date. Second best is the Al_2O_3/SiO_2 combination. The Y_2O_3/SiO_2 combination is very discouraging. The differences between the calculated and measured curves for high reflectors, in general, can be due to absorption, scattering, layer thickness variations and refractive index variations. Layer thickness variations were ruled out for this work by separate measurements and Monte Carlo computer calculations. Refractive index variations and absorption/scattering will be described in the Discussion section of this report.

Single Layer Optical Properties

Fabrication of multilayer mirrors in the ultraviolet requires very close attention to the onset of the absorption edge of each coating material, enhanced scattering effects because of the very short wavelengths, and refractive index dispersion near the absorption edge. The absorption edge for each material can be seen in Figure 13 which displays typical spectrophotometer data for single layer coatings of HfO_2, Y_2O_3 and Al_2O_3 on fused silica substrates. The transmission of the bare substrate used for each coating is also shown. Except for the SiO_2 coatings which transmit very well down to and below 200 nm, Al_2O_3 by far has the shortest wavelength absorption edge. The actual edge for the Al_2O_3 coating is probably below 200 nm, but appears to be at a higher wavelength in Figure 13 because of absorption by the SiO_2 substrate. Suprasil type silica should be used for future ultraviolet work rather than the type IR-12 used for these measurements. The absorption edges for Y_2O_3 and HfO_2 both are seen to be near 220 nm. However, some transmission loss due to absorption and/or scattering is apparent for each material near the 248 nm wavelength of interest.

Absorption and scattering losses for each coating material can be seen more clearly in Figures 14 through 17 which show the difference between coated and uncoated substrate transmission near 248 nm as a function of single-layer coating thickness. Data plotted here are taken from coatings on both PNL and LLNL substrates. The thickness corresponding to a quarter wavelength at 248 nm is also shown. These losses are due to both absorption and scattering, and separation of the contributions made by each is, in general, difficult. However, Figures 14 through 17 can be used to make rough estimates. For thin films which are polycrystalline (such as HfO_2, Y_2O_3 and Al_2O_3 as shown in the next section) both absorption and scattering losses are expected to increase with thickness. For glassy films (such as SiO_2) only the absorption loss is expected to increase significantly with thickness. The transmission loss ΔT due to absorption, in general, increases as

$$\Delta T \sim (1-e^{-\beta x}),$$

where β is the absorption coefficient and x the coating thickness. For thin films, the loss is approximatley given by

$$\Delta T \sim \beta x,$$

where β is the slope of a transmission loss versus thickness plot. Thus for the case of SiO_2, where scattering is assumed to be negligible, a least squares straight-line fit to the data of Figure 17 yields β (248 nm) = 210 cm^{-1}. Upper limits for β (248 nm) for HfO_2, Y_2O_3 and Al_2O_3 can be similarly deduced from Figures 14 through 17 if it is assumed that scattering does not increase with thickness. The results listed in Table 4 are 2600, 1770 and 3900 cm^{-1} for Al_2O_3, Y_2O_3 and HfO_2, respectively. Note that these coefficients are 10 times larger than β for SiO_2, suggesting that, rather than being insignificantly small, the scattering contribution to the transmission loss is in fact much larger than the absorption contribution. However, the upper limits calculated for β of these three polycrystalline coatings will be useful in the Discussion section of this report. Also shown in Table 4 for each coating material is the extinction coefficient or imaginary part of the refractive index k defined as

$$k = \beta\lambda/4\pi.$$

Note that like β, k for HfO_2, Y_2O_3 and Al_2O_3 is an upper limit value.

The refractive index for each coating material can be deduced from the amplitude of oscillation for transmission data such as that displayed in Figure 13. Refractive index dispersion can be calculated from the positions of the extrema. Figure 18 shows the variation of the refractive index with wavelength for each coating material, and Table 5 lists fit parameters for a least squares analysis of data taken for several coatings of each material. The difference in absorption edge between SiO_2 and Al_2O_3 compared to Y_2O_3 and HfO_2 is obvious from the rate of variation of the index in Figure 18. The refractive index for each coating material can be calculated at any wavelength from the fit parameters and the equation given in Table 5. Column 5 of the table lists the index at 248 nm. Column 4 is a good estimate of the long wavelength (~ 1000 nm) index.

Coating Microstructural Properties

Coating microstructural properties deduced from x-ray diffractometer data are summarized for all four materials in Table 6. Properties deduced include crystal structure, grain size and preferred crystallographic orientation of grains relative to the substrate surface.

SiO_2 coatings made in this work were glassy or amorphous, and exhibited no long range order. Grain size and preferred orientation have little meaning in this limit.

Al_2O_3 coatings made in this work crystallized in the cubic (γ) structure with grain sizes of 30 to 100 Å. Orientation of the grains was random.

Y_2O_3 coatings had the largest grain sizes of all materials examined in this work, and ranged from 340 to 540 Å. The grains were very strongly oriented with the (222) crystallographic planes parallel to the substrate surface. The ratio of the area under the (222) peak to the sum of the areas for all the diffraction peaks was typically 0.90.

HfO_2 coatings crystallized in the monoclinic structure with grain sizes of 100 to 300 Å. The preferred orientation was $(11\bar{1})$, and was strong with a peak area ratio typically of 0.65.

DISCUSSION

Overview

From the results presented in the previous section it seems clear that the principal factor limiting the damage thresholds observed for mirrors made to date is their relatively low reflectivity. It is well known that reflectivity losses in all-dielectric mirrors are due to four factors: (1) absorption, (2) scattering, (3) layer thickness errors, and (4) refractive index errors due to layer-to-layer variation or dispersion. With the extensive characterization data accumulated in this work, each of these factors can be related to either the optical or physical properties of the individual coating materials or to the process used to deposit them. In the paragraphs that follow, the loss in reflectivity due to each of these factors is estimated in magnitude for each coating material combination examined, and the coating properties or deposition process features responsible for each factor is discussed. In general, it is found that the relative size of each factor for each material combination is different, so that each combination will require individual optimization in any future work contemplated.

Table 7 summarizes the reflectivities achieved for typical HfO_2/SiO_2, Y_2O_3/SiO_2 and Al_2O_3/SiO_2 mirrors, and lists the estimated reflectivity losses due to transmission, absorption and scattering as a function of the tuned wavelength of the mirror. Both good and bad reflectors are included to give a better overall picture. The transmission losses were made by direct spectrophotometer measurements for mirrors made on fused silica substrates which transmit well near 248 nm. Losses due to transmission are primarily caused by thickness and refractive index errors since all reflectors were made with a sufficient number of layers to limit transmission to 0.1% for HfO_2/SiO_2 and Y_2O_3/SiO_2 and to 0.8% for Al_2O_3/SiO_2. The combined absorption plus scattering loss labeled A+S in column 6 of Table 7 was calculated by summing the reflectivity and transmission measured at the tuned wavelength and subtracting from 100%. The absorption loss labeled A in column 7 was calculated from the extinction coefficients k of Table 4 and the refractive indices n of Table 5 using the relation[1]

$$A = -\delta R = \frac{2\pi}{n_H^2 - n_L^2}\,(k_H + k_L).$$

For each calculated A loss, L refers to SiO_2 and H to either HfO_2, Y_2O_3 or Al_2O_3. Although the k values of Table 4 are upper limits, their use allows calculation of an upper limit for A so that the losses due to absorption and scattering can be separated for complete analysis of the reflectors.

HfO_2/SiO_2 Mirrors

Best reflectors to date were obtained for HfO_2/SiO_2. As shown in Table 7, reflectivities in excess of 99% were obtained at some points on some mirrors. At these points, the principal losses were 0.6 to 0.9% and were due to mirror transmission, indicating that slightly better control of layer thickness and/or refractive index is needed to attain the 0.1% minimum theoretical loss. The index dispersion data of Figure 18 and our experience with the degree of thickness control achievable with the sputtering process suggest that this small problem is due mainly to accounting for the rapid wavelength variation of the refractive index with insufficient accuracy. The large dispersion in the index of HfO_2 is due to its relatively low optical band gap. The difficulty it presents must be traded off against the advantages of the high refractive index of this material. Note that absorption losses at the high reflectivity regions were at most 0.1 to 0.2%, indicating that the absorption edge of HfO_2 is sufficiently low in wavelength for use of this material at 248 nm. At some regions of HfO_2/SiO_2 mirrors, reflectivities were only ~ 95%. As shown in Table 7, the transmission loss at these points was 1% and about the same as in the high reflectivity regions of the mirrors. However, the absorption plus scattering loss was 3.6%. Using the calculated upper limit of 1.5% for absorption loss, most (2.1%) of the reflectivity loss is seen to arise from scattering. Scattering losses are caused by coating surface roughness and by nonhomogeneous coating microstructure due to columnar grains or growth features.

It is interesting to note that with HfO_2/SiO_2, and with Y_2O_3/SiO_2 and Al_2O_3/SiO_2 as will be discussed later, the high reflectivity regions were almost always near the perimeter of the two-inch substrates and the lower reflectivity regions near the central 1/2 inch. An example of a typical reflectivity and tuned-wavelength profile is shown in Figure 19. The cause of the increased surface roughness near the center of the mirrors is not understood. A similar center roughening phenomenon was observed several times for single-layer HfO_2 coatings deposited at high gas pressures. The increased roughness appears to be

an artifact of the sputter deposition of these particular materials and may be due to negative ion effects during deposition in the plasma. Further discussion of negative ion effects is beyond the scope of this report.

One general feature of the HfO_2 coatings that also deserves mention is the grain size. As shown in Table 6, grain sizes ranged from 100 to 300 Å. Although scattering losses due to surface roughness were not observed to be large, with the exception of the peculiar phenomenon mentioned above for the central region of the mirrors, future work on HfO_2 coatings for ultraviolet applications should address further reduction of grain size through deposition parameter optimization since ideal coating surface topographies are obtained with the smallest grain sizes. Data supporting this conclusion are shown in Figure 20 which displays the grain-size dependence of the scattering loss at 248 nm for single-layer coatings with near-equal thicknesses of approximately 2500 Å.

Y_2O_3/SiO_2 Mirrors

The least encouraging results to date were obtained for Y_2O_3/SiO_2. As shown in Table 7 and Figure 9, reflectivities ranged from 55 to 83% and were strongly dependent on tuned wavelength. Highest reflectivities occurred for the longest tuned wavelengths. The poor performance of Y_2O_3/SiO_2 reflectors is difficult to understand because the single-layer Y_2O_3 coatings exhibited excellent optical properties. The data of Figure 13 show very little loss near 248 nm, and the maximum 248 nm extinction coefficient in Table 4 is the lowest of the three high index materials. The absorption edge shown in Figure 13, however, is slightly longer in wavelength than expected and even falls at longer wavelengths than HfO_2. Largest reflectivity losses come from absorption plus scattering, as shown in Table 7, and range from 13 to 32%. The maximum calculated absorption loss for an Y_2O_3/SiO_2 reflector is 1.0%, suggesting that scattering is the principal problem. The transmission losses shown in Table 7 are also very large, but probably result from the large scattering losses rather than from thickness or index errors. A contribution due to refractive index errors associated with the large dispersion of Y_2O_3, however, should not be completely ruled out.

There are several apparent explanations for the large scattering losses. First the grain sizes shown in Table 6 for Y_2O_3 coatings are 340 to 540 Å. These grains are very large for ultraviolet applications and almost certainly result in extreme surface roughness. The very strong preferred crystallographic orientation of the Y_2O_3 coatings suggests pronounced columnar microstructure with surface roughness caused by the rounded caps of the columnar grains. In fact, some SEM surface micrographs such as that displayed in Figure 21 for a 23-layer high reflector show the columnar caps or "cobblestone effect" very clearly. Secondly, the possibility of a metallurgical reaction between the SiO_2 and Y_2O_3 layers during deposition is suggested by the apparent difference in optical properties for single layers and multilayer stacks. Several Y-Si compounds exist in the published phase diagrams[2] and may be thermodynamically likely under the conditions of coating deposition. Finally, the center roughening phenomenon described for HfO_2/SiO_2 was equally apparent in the Y_2O_3/SiO_2 mirrors.

Al_2O_3/SiO_2 Mirrors

Reflectivities for Al_2O_3/SiO_2 ranged from 74 to 90%, and were typically 80 to 88%. Results shown in Table 7 for three of the best Al_2O_3/SiO_2 mirrors indicate that transmission, absorption and scattering losses were equally important and were each typically 5%. Recall, however, that the absorption loss is a calculated maximum value so that the actual scattering loss may have been greater than 5% but less than 10%. Most of the large transmission loss is believed to result from the smallness of the refractive index contrast between Al_2O_3 and SiO_2 which results in a very narrow reflectance peak (see Fig. 10) and requires unusually tight tolerances on index reproducibility from layer to layer and run to run. Recall that 0.8% of the transmission loss is expected since the Al_2O_3/SiO_2 mirrors were designed for only 99.2% reflectivity. The scattering loss most likely results from the large number of coating layers required for Al_2O_3/SiO_2 and the larger thickness of each layer for these low index materials. In fact, the Al_2O_3/SiO_2 reflector is 1.68 μm thick, which is almost twice the 0.898 μm thickness of the Y_2O_3/SiO_2 reflector and almost three times the 0.599 μm thickness of the HfO_2/SiO_2 reflector. This increase in thickness offsets the surface-roughness benefits of the very fine grain size of the Al_2O_3 coatings, shown in Table 6 to be only 30 to 100 Å. Future work with Al_2O_3/SiO_2 should examine

tradeoffs between reflectivity and scattering for stacks with different numbers of coating pairs. The actual absorption loss in the Al_2O_3/SiO_2 stack is believed to be significantly less than 5% because of the large band gaps of these materials. Finally, some reduction of reflectivity near the center of the two-inch substrates was also noticed for Al_2O_3/SiO_2, but the effect appeared to be smaller than for HfO_2/SiO_2 and Y_2O_3/SiO_2.

CONCLUSIONS

Laser damage thresholds of 2.0 to 2.3 J/cm^2 for 20 ns pulses at 248 nm were consistently demonstrated for all-dielectric reflectors made with a 39-layer quarter-wave stack of Al_2O_3/SiO_2 plus a half-wave SiO_2 underlayer and a half-wave SiO_2 overlayer. A threshold of 2.1 J/cm^2 was achieved for one 13-layer stack of HfO_2/SiO_2, but two other identical reflectors damaged at 0.9 and 1.0 J/cm^2. Thresholds for 21-layer Y_2O_3/SiO_2 reflectors ranged from 0.3 to 1.1 J/cm^2. The HfO_2/SiO_2 and Y_2O_3/SiO_2 reflectors also employed half-wave SiO_2 underlayers and overlayers. Although short of the 5 J/cm^2 goal of this work, optimization of the deposition of these coating materials to reduce surface roughness and scattering promises to yield higher thresholds.

Point-to-point average reflectivities of 94-96% were achieved for HfO_2/SiO_2 reflectors, with 99-100% reflectivities at some points. Al_2O_3/SiO_2 mirrors averaged 80-83% with some 90% points. Y_2O_3/SiO_2 reflectors averaged 62-80% with some 85% points. The principal cause of reduced reflectivity in most cases was scattering from surface roughness. The easiest reflectors to make were the HfO_2/SiO_2 because the high refractive index contrast of this combination requires fewer and thinner coating layers and results in a broad reflectance maximum. Al_2O_3/SiO_2 mirrors were the most difficult to make because of low refractive index contrast.

Damage threshold did not correlate with the mirror reflectivity, although it seems likely that improvement of the mirror reflectivity by reduction of obvious coating surface roughness would produce the most immediate improvement in damage resistance. Damage thresholds for reflectors were similar to those obtained with single layers of the high-index material, supporting the conclusion stated in the previous sentence. No clear evidence for damage initiation by

two-photon processes was obtained from the dependence of threshold on the absorption edges of the three high-index materials, although Al_2O_3 did consistently exhibit the highest damage resistance. Damage resistance did not appear to depend on: (1) single-layer thickness, (2) stack tuned wavelength, (3) laser beam polarization, (4) substrate polishing technique, or (5) substrate cleaning technique. It did appear, however, that significant improvement in damage resistance could come from increased attention to coating cleanliness.

SiO_2, Al_2O_3, Y_2O_3 and HfO_2 all appear to be promising candidate materials for use at 248 nm wavelength. However, further optimization of coating properties is definitely necessary for the three high-index materials. HfO_2 and Y_2O_3 must be deposited with finer grain sizes to reduce surface roughness. The peculiar center roughening phenomenon, which appears to be an artifact of the reactive sputter deposition of these materials, must be eliminated or minimized for HfO_2, Y_2O_3 and Al_2O_3. The possibility of a metallurgical reaction between Y_2O_3 and SiO_2 was suggested by the difference in optical properties for Y_2O_3 in single layers and Y_2O_3 in multilayer stacks with SiO_2. Finally, the large coating thickness for Al_2O_3/SiO_2 reflectors suggests study of the tradeoff between reflectivity and scattering as the number of coating pairs is varied.

The principal factor influencing the apparent ultraviolet absorption edge for each of HfO_2, Y_2O_3 and Al_2O_3 was scattering due to coating surface roughness and large microstructural characteristics such as grain boundaries and columnar growth features. Scattering contributed by substrate roughness did not appear to be significant. The influence of absorption on the ultraviolet edge appeared to be small. Thus the level of stoichiometry and purity achieved appear to be adequate, and absorption due to intrinsic interband mechanisms does not appear to be important for any of these materials at 248 nm.

Reactive sputter deposition appears to be a viable technique for fabricating all-dielectric ultraviolet reflectors. A deposition parameter matrix study is, however, required to optimize coating microstructure and surface topography. Increased attention to coating thickness and index control from layer-to-layer and run-to-run also seems important for ultraviolet reflectors. Refinement of refractive index dispersion curves and their incorporation in multilayer coating designs is further needed. Finally, the level of cleanliness achieved in coating deposition and the care in handling of finished coatings require improvement.

RECOMMENDATIONS FOR FUTURE STUDY

The most important area for future work is optimization of the microstructure and surface topography of the high-index materials HfO_2, Y_2O_3 and Al_2O_3 to minimize reflectivity losses due to scattering and thus increase damage resistance. Such optimization should probably take the form of a deposition parameter matrix study and should include deposition rate, substrate temperature, sputtering gas pressure and substrate bias, all of which are known to influence coating microstructure in generally predictable ways. Appropriate coating evaluation techniques for the matrix study would include ultraviolet transmission measurements to determine the spectral dependence of the absorption edge, x-ray diffraction for grain size and orientation, and SEM for direct observation of surface features. Fabrication of multilayer stacks is also required to confirm coating improvements, and ultimately laser damage testing should be done.

Deposition experiments aimed at understanding the center roughening phenomenon should also be carried out. Particular attention should be paid to negative ion bombardment of the growing film in the sputtering plasma. These experiments should include examination of the influence of target voltage, sputtering gas pressure, substrate-target spacing, and off-axis placement of the substrate. Many aspects of the microstructure optimization and negative ion experiments can thus be investigated simultaneously.

Procedures resulting in tighter tolerances for layer thickness and refractive index control and monitoring with the sputtering process should be investigated, accompanied by Monte Carlo computer simulations to deduce the magnitude of expected effects. Refined refractive index dispersion curves are also needed, and an improved method for their incorporation into coating design should be developed.

Improvement in coating overall cleanliness is needed, and more attention should be paid to "cosmetics". Substrate cleaning procedures require further development, as do procedures for ensuring a cleaner vacuum deposition environment and more careful handling of completed coatings.

For the Al_2O_3/SiO_2 system, and possibly also HfO_2/SiO_2 and Y_2O_3/SiO_2, the influence of the number of coating pairs on reflectivity improvement and scattering losses should be examined.

Finally, consideration should be given to expanding this effort to include improved compositions such as Zr-free HfO_2 or cubic-stabilized HfO_2• 15 mole % Y_2O_3. These compositions may provide reduced absorption and scattering in the ultraviolet. New materials such as $MgAl_2O_4$, $Y_4Al_2O_9$ and Sc_2O_3 should also be studied for use as the high-index material. Considerable data on the former two materials is already available[3].

ACKNOWLEDGEMENTS

The authors would like to express their gratitude for the opportunity to work with the enthusiastic and capable staff at Lawrence Livermore National Laboratory on the development of damage resistant coatings for Kr*F lasers. In particular we thank Howard Lowdermilk, Dave Milam and Frank Rainer for making this work possible and for their time and efforts in testing and evaluating PNL coatings. We also thank Frank Rainer for his excellent summary chart and table which appear as Fig. 2 and Table 3 in this report. Finally, thanks are due to H.E. Kjarmo of PNL for SEM, x-ray diffraction and x-ray fluorescence analysis of the coatings.

REFERENCES

1. J.A. Dobrowolski, in Handbook of Optics, edited by Walter G. Driscoll and William Vaughan, (McGraw-Hill, New York 1978), p. 8-65.

2. R.P. Elliott, Constitution of Binary Alloys, First Supplement, (McGraw-Hill, New York 1965), p. 823.

3. W.T. Pawlewicz, D.D. Hays and P.M. Martin, Thin Solid Films 73 (1980) 169-175.

TABLE 1: Vendor, Fabrication Method and Purity Of Sputtering Targets

Material	Vendor	Fabrication Method	Purity
SiO_2	Heraeus-Amersil, Inc.	Suprasil 2 Fused Silica	99.9999%
Al	Materials Research Corp.	VP Metal plate	99.995%
Y_2O_3	Cerac, Inc.	Hot-pressed powder	99.999%
HfO_2	Cerac, Inc.	Hot-pressed powder	99.95%, except for 3 mole % ZrO_2

TABLE 2: Sputter Deposition Conditions For All Coatings Damage Tested

LLNL Substrate#	Damage Test #	PNL Coating	Coating Material	Coating Design	Substrate Clean	Target Power(W)	Target Volts	Gas Pressure (mtorr)	Ar/O_2 (%)	Deposition Rate (Å/min)
804	14	11 D	Al_2O_3	λ/2	D + S	600	1550	20	85/15	95.9
805	15	11 E	"	"	D	"	1450	"	"	102
811	18	12 D	"	"	D	"	1400	"	50/50	81.7
812	19	12 E	"	"	D + S	"	1400	"	"	80.9
808	12	11 B	"	3λ/2	D	"	1550	"	85/15	87.5
803	13	11 C	"	"	D + S	"	1550	"	"	85.5
807	16	12 B	"	2λ	D	"	1400	"	50/50	70.6
809	17	12 C	"	"	D + S	"	1350	"	"	70.1
2504	95	14 C	Al_2O_3/SiO_2	$SLL(HL)^{19}HLL$	D + S	600/600	1650/800	20	50/50	48.4/122
2505	96	14 D	"	"	D + S	"	1650/800	"	50/50	"
2514	97	14 H	"	"	D + S	"	1600/700	"	"	78.8/123
2515	98	14 I	"	"	D + S	"	1600/700	"	"	"
806	22	11 D	HfO_2	λ/2	D + S	600	700	100	90/10	63.4
810	23	11 E	"	"	D + S	"	650	"	"	62.3
813	20	11 B	"	2λ	D + S	"	800	"	"	54.9
814	21	11 C	"	"	D + S	"	700	"	"	65.2
3018	94	12 C	"	"	D + S	"	650	20	85/15	79.0
2519	104	13 D	HfO_2/SiO_2	$SLL(HL)^{6}HLL$	D + S	600/600	850/550	20	85/15	93.5/125.6
2591	105	13 F	"	"	D + S	"	850/575	"	"	"
2592	106	13 G	"	"	D + S	"	875/550	"	"	"
3043	93	11 D	Y_2O_3	λ/2	D + S	600	900	20	85/15	97.4
3022	91	11 B	"	2λ	D + S	"	900	20	"	92.6
3032	92	11 C	"	"	D + S	"	900	20	"	92.9
2517	99	12 C	Y_2O_3/SiO_2	$SLL(HL)^{10}HLL$	D + S	600/600	1000/700	20	85/15	90.4/127.7
2517	100	12 H	"	"	D + S	"	1050/600	"	"	"
2518	101	12 E	"	"	D + S	"	1100/675	"	"	"
2518	102	12 G	"	"	D + S	"	1050/625	"	"	"
2520	103	12 I	"	"	D + S	"	1050/650	"	"	"

TABLE 3: Damage Threshold Of PNL Sputtered Coatings At 248 nm, 20 ns

LLNL Substrate#	Damage Test#	PNL Coating#	Coating Material	Coating Design	O_2 %	λ nm	R %	Sub-strate	Substrate Polish/Prep.	Beam Polar.	Comments	Clean 0-3	Threshold J/cm²
804	14	11 D	Al_2O_3	λ/2	15			FS	Rear, D+S	s		1	1.6 ± 0.2
805	15	11 E	"	"	15			"	D	s		1	1.7 ± 0.2
811	18	12 D	"	"	50			"	D	s	Large flaws	1	2.6 ± 0.4
812	19	12 E	"	"	50			"	D+S	s		0	3.2 ± 0.3
808	12	11 B	"	3λ/2	15			"	D	s	Voids,droplets	2	1.7 ± 0.2
803	13	11 C	"	"	15			"	D+S	s	Thresh. cracks	2	2.1 ± 0.2
807	16	12 B	"	2λ	50			"	D	s		2	1.9 ± 0.2
809	17	12 C	"	"	50			"	D+S	s		1	1.5 ± 0.2
2504	95	14 C	Al_2O_3/SiO_2	$SLL(HL)^{19}HLL$		248	81	BK-7	D+S	p		2	2.3 ± 0.2
2505	96	14 D	"	"		255	83	"	D+S	p	Scuffs, green thresh.	2	2.0 ± 0.2
2514	97	14 H	"	"		249	83	"	Rear, D+S	p		2	2.3 ± 0.2
2515	98	14 I	"	"		257	80	"	Rear, D+S	p		2	2.3 ± 0.2
806	22	11 D	HfO_2	λ/2				FS	D+S	s	Yellow edge	2	0.5 ± 0.1
810	23	11 E	"	"				"	D+S	s		2	0.5 ± 0.1
813	20	11 B	"	2λ				"	D+S	s	Colored edge, fog	3	0.8 ± 0.2
814	21	11 C	"	"				"	D+S	s	Splotched, fog	3	0.7 ± 0.1
3018	94	12 C	"	"				"	Super, D+S	p	Splotched, very foggy	3	0.3 ± 0.1
2519	104	13 D	HfO_2/SiO_2	$SLL(HL)^{6}HLL$		249	96	BK-7	D+S	p		3	2.1 ± 0.2
2591	105	13 F	"	"		266	96	"	D+S	p	Vague Threshold	2	0.9 ± 0.1
2592	106	13 G	"	"		253	94	"	D	p	Vague Threshold	2	1.0 ± 0.4
3043	93	11 D	Y_2O_3	λ/2				FS	Super, D+S	p		1	1.1 ± 0.1
3022	91	11 B	"	2λ				"	Super, D+S	p		3	0.6 ± 0.1
3032	92	11 C	"	"				"	Super, D+S	p	Artifacts damage	3	< 0.3
2517	99	12 C	Y_2O_3/SiO_2	$SLL(HL)^{10}HLL$		258	67	BK-7	D+S	p	Droplets	2	0.4 ± 0.2
"	100	12 H	"	"		244	62	"	Rear, D+S	p	Smudges	2	0.6 ± 0.2
2518	101	12 E	"	"		280	80	"	D+S	p	Scuffs	2	0.5 ± 0.1
"	102	12 G	"	"		247	67	"	Rear, D+S	p		1	0.6 ± 0.3
2520	103	12 I	"	"		252	73	"	D+S	p		0	0.7 ± 0.1

TABLE 4: Absorption And Extinction Coefficients At 248 nm For Each Coating Material Deduced From Figures 12 through 15. The Values For HfO_2, Y_2O_3, and Al_2O_3 Are Upper Limits As Explained In The Text.

Coating Material	β(248nm) (cm^{-1})	k(248nm)
SiO_2	210	.00041
Al_2O_3	2600	.0051
Y_2O_3	1770	.0035
HfO_2	3900	.0077

TABLE 5: Fit Parameters For Least Squares Analysis Of Refractive Index Dispersion According To The Relation $n^2 = 1 + \frac{A}{1-B/\lambda^2}$

Material	A	B	$(1+A)^{1/2}$	n(248nm)
SiO_2	1.0931	6599	1.447	1.491
Al_2O_3	1.7035	8236	1.644	1.722
Y_2O_3	2.4261	20912	1.851	2.162
HfO_2	2.8557	23545	1.964	2.372

TABLE 6: Microstructural Properties Deduced From X-Ray Diffractometer Data For Single Layers.

Material	Crystal Structure	Grain Size (Å)	Preferred Orientation
SiO_2	Glassy	Glassy	-----
Al_2O_3	Cubic (γ)	30 - 100	Random
Y_2O_3	Cubic	340-540	(222) v. str. (.90)
HfO_2	Monoclinic	100-300	$(11\bar{1})$ str. (.65)

TABLE 7: Transmission And Absorption/Scattering Losses For High Reflectors With Tuned Wavelengths Near 248 nm Made From Three Coating Material Combinations.

Coating Materials	PNL Coating#	λ_o (nm)	R(λ_o) (%)	T(λ_o) (%)	A+S(λ_o) (%)	A(λ_o)* (%)
HfO_2/SiO_2	13 E-4	225	95.4	1.0	3.6	1.5
	13 E-1	225	99.0	0.9	0.1	1.5
	13 J	228	99.2	0.6	0.2	1.5
Y_2O_3/SiO_2	11 M	237	55.0	12.8	32.2	1.0
	12 B-1	258	64.7	5.9	29.4	1.0
	11 L	259	81.8	4.6	13.6	1.0
	12 B-2	263	78.2	4.6	17.2	1.0
	11 J	269	83.3	1.5	15.2	1.0
	11 K	270	81.7	5.5	12.8	1.0
Al_2O_3/SiO_2	13 B-1	227	87.6	8.2	4.2	4.7
	14 B	228	86.0	6.6	7.4	4.7
	13 B-2	230	86.1	3.7	10.2	4.7

* Calculated maximum value

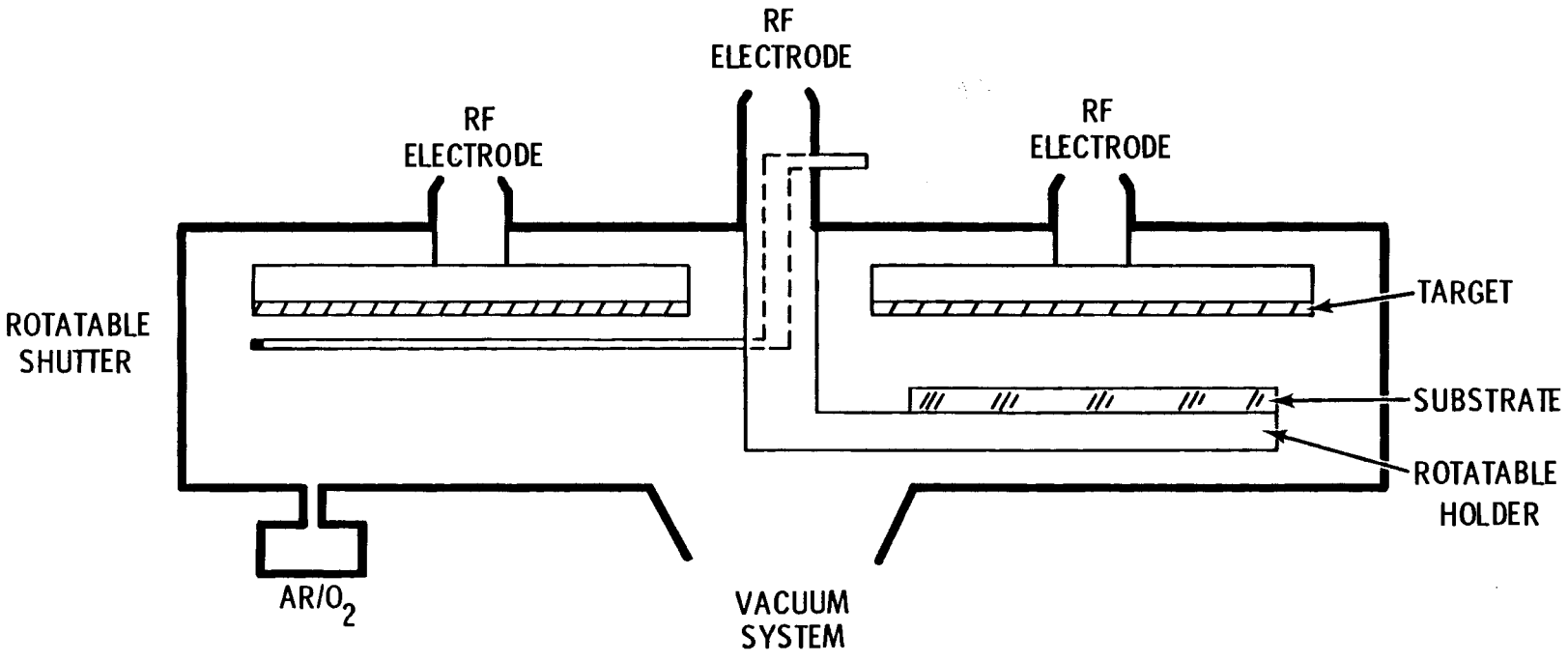

Figure 1. Schematic diagram of rf diode sputtering system used for coating deposition.

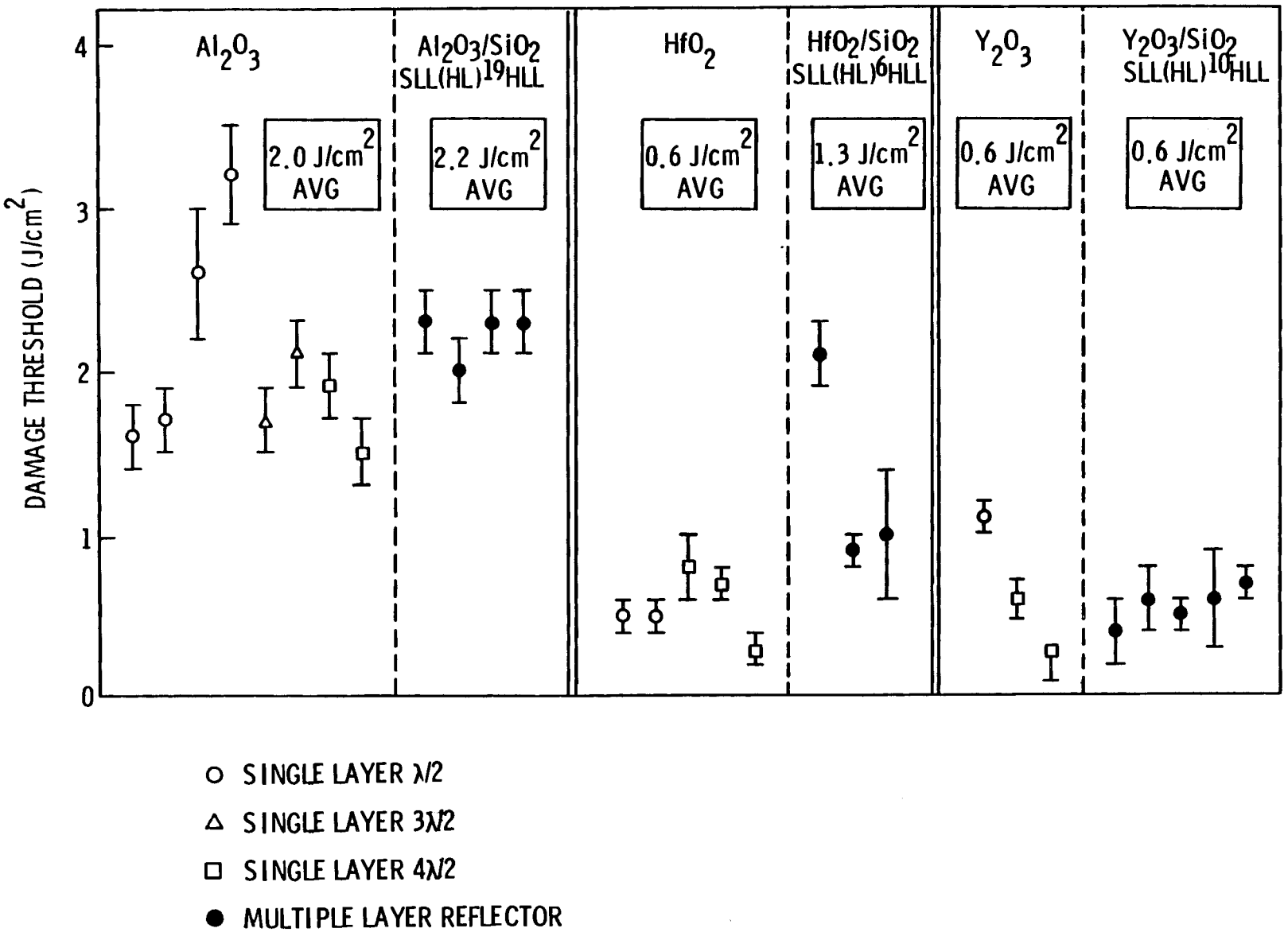

Figure 2. Damage thresholds of PNL sputtered coatings at 248 nm, 20 ns.

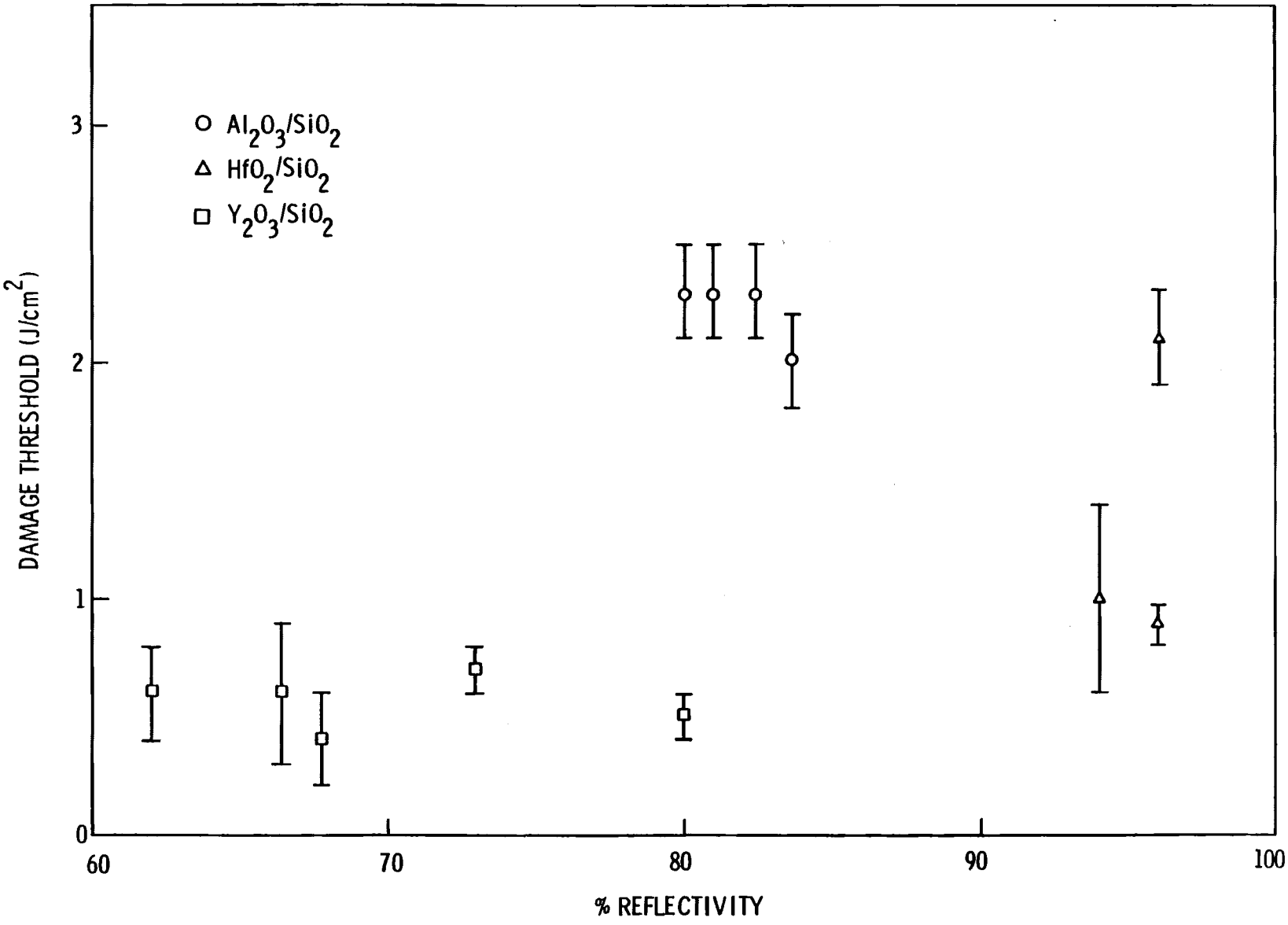

Figure 3. Lack of correlation between damage threshold and mirror reflectivity.

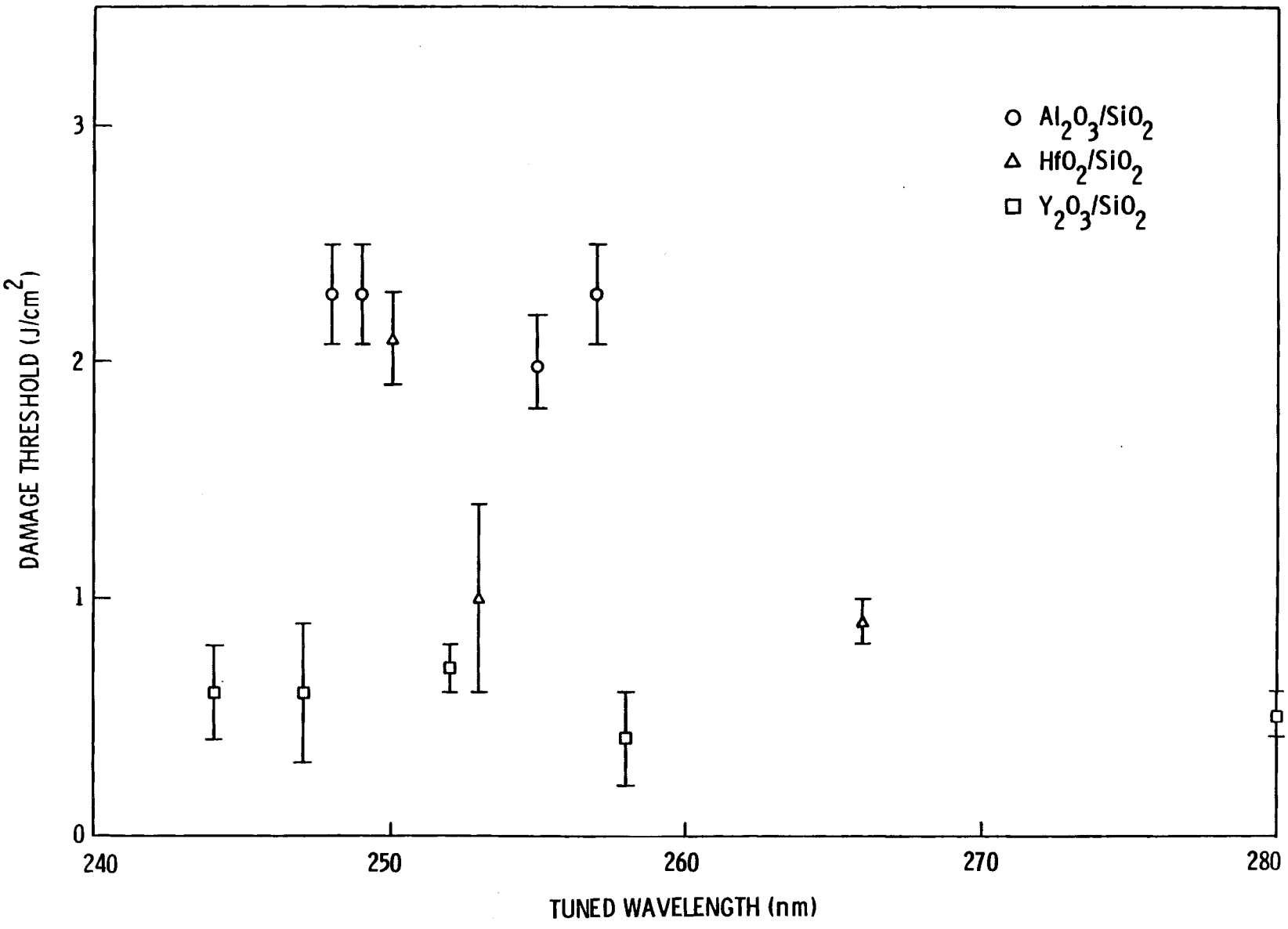

Figure 4. Lack of correlation between damage threshold and mirror tuned wavelength.

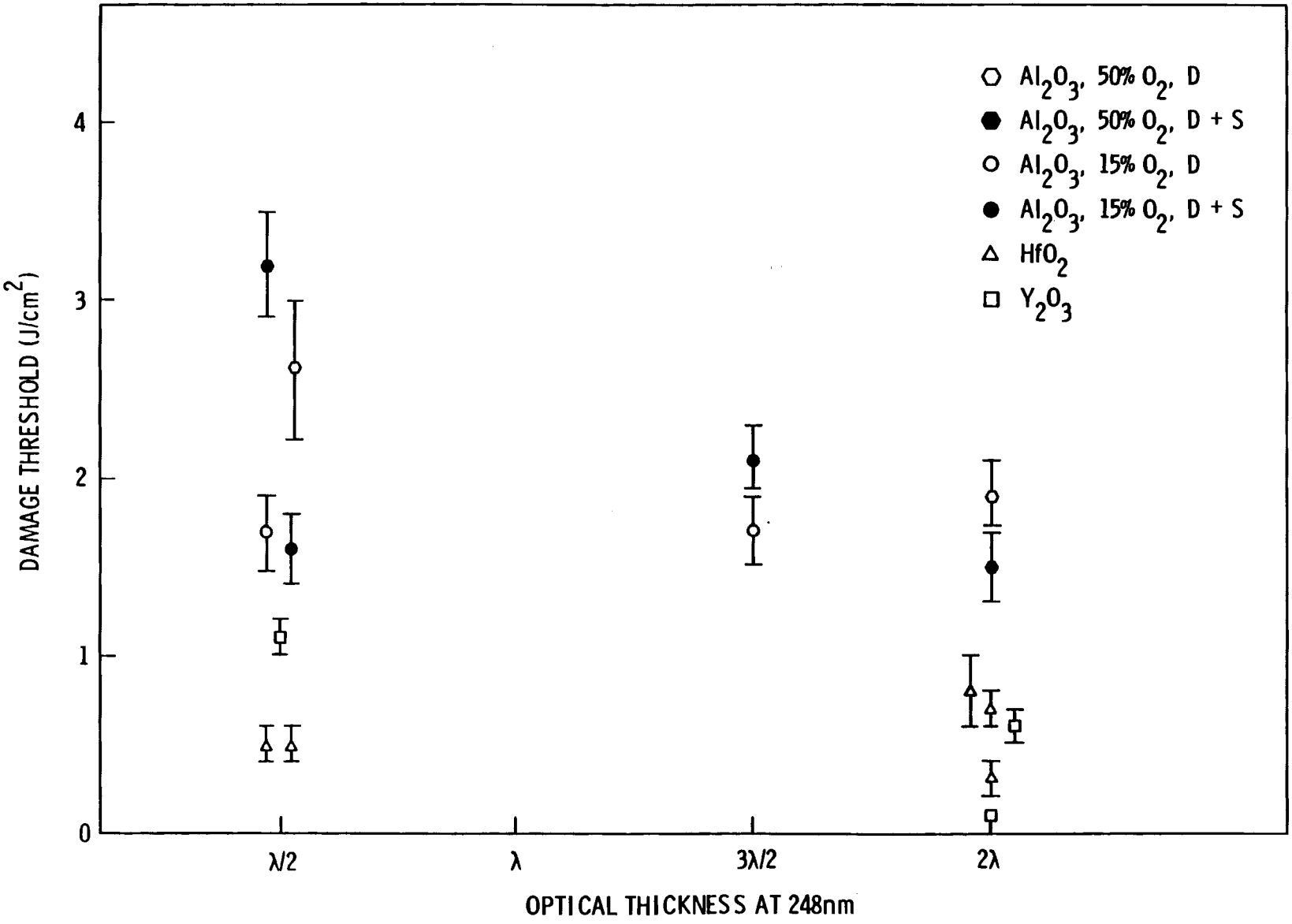

Figure 5. Lack of correlation between damage threshold and single-layer coating thickness, O_2 partial pressure or substrate cleaning procedure.

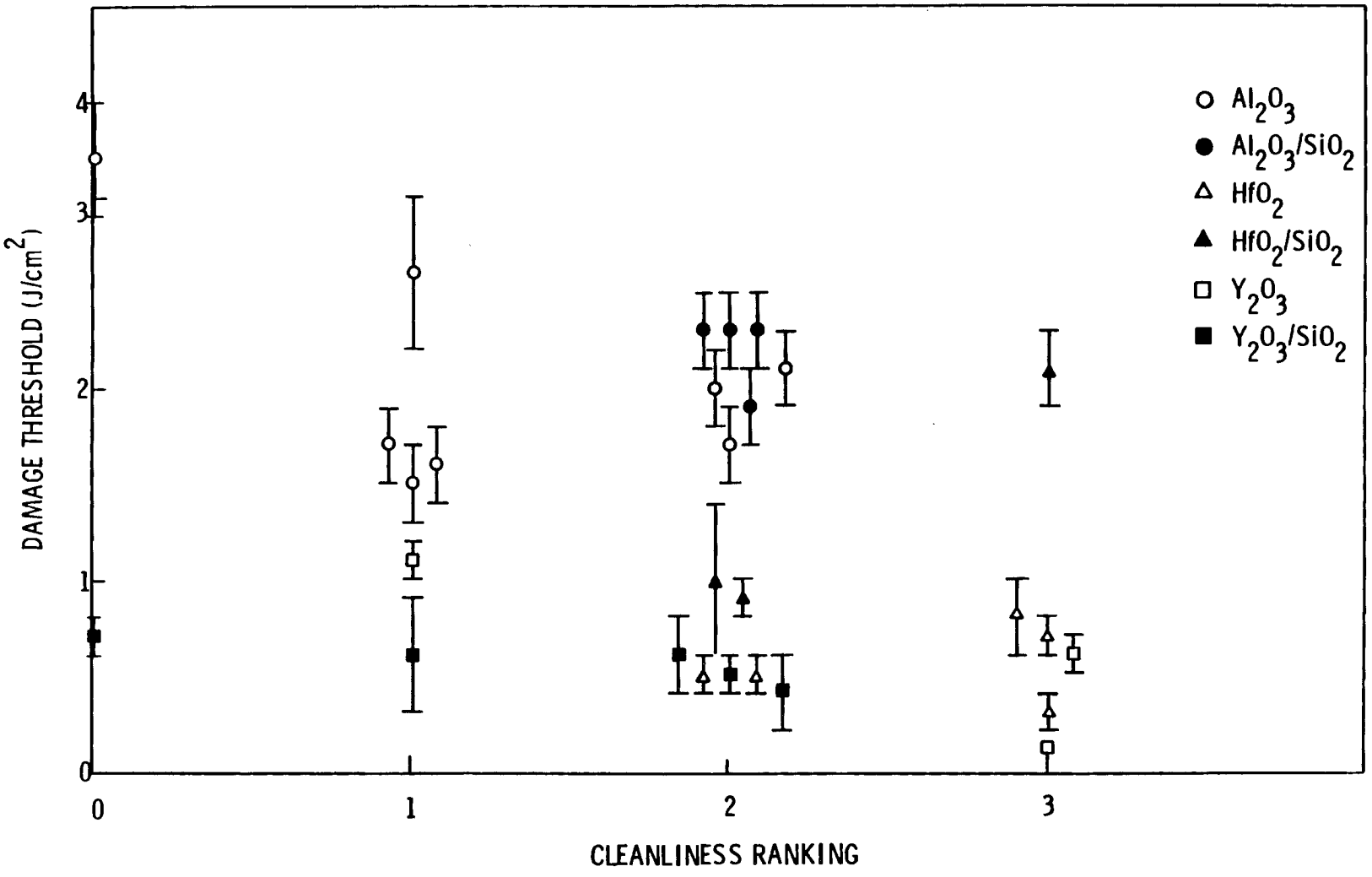

Figure 6. Intragroup correlation between damage threshold and coating "cleanliness" ranking.

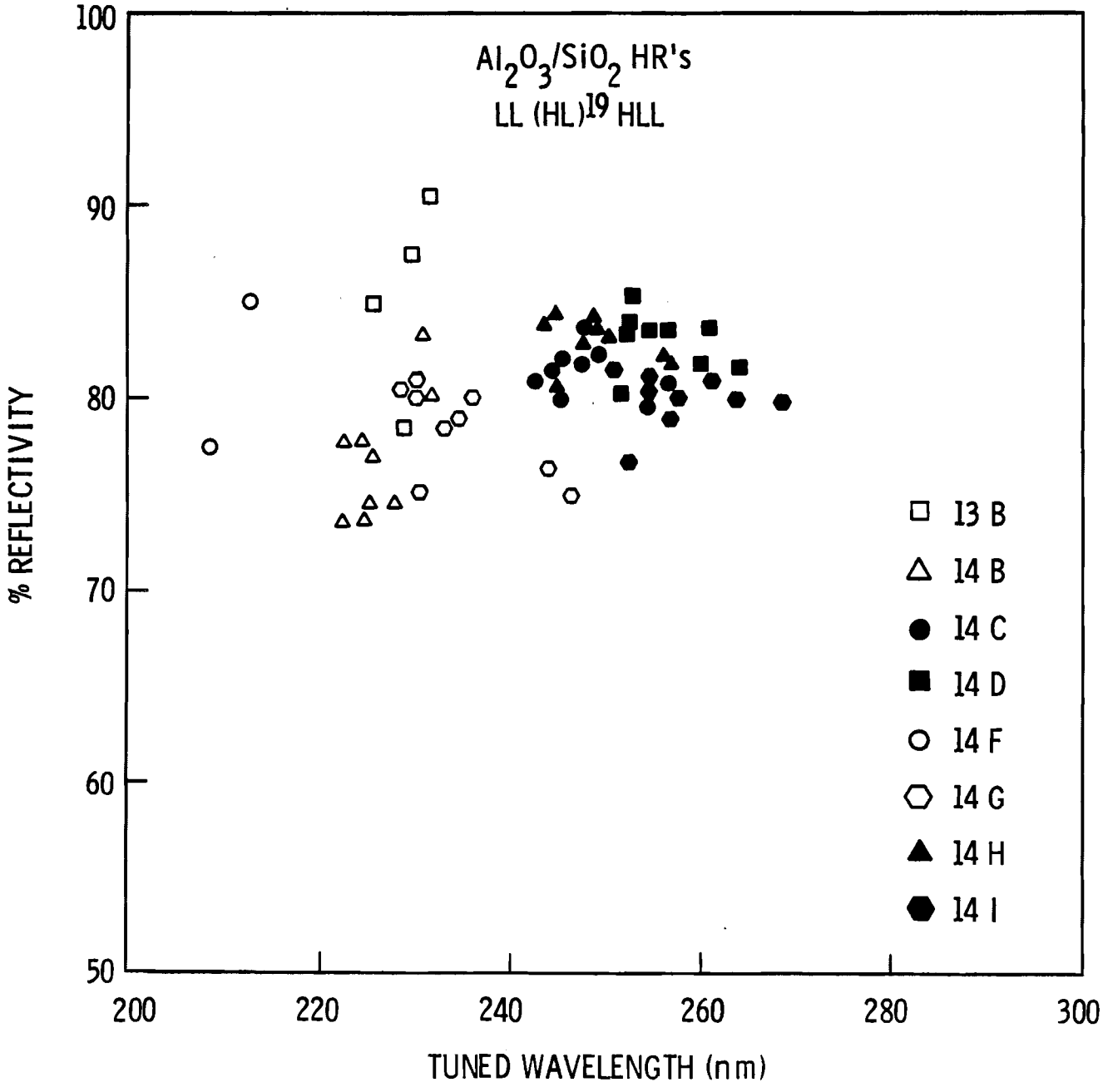

Figure 7. Variation of reflectivity of Al_2O_3/SiO_2 mirrors with tuned wavelength.

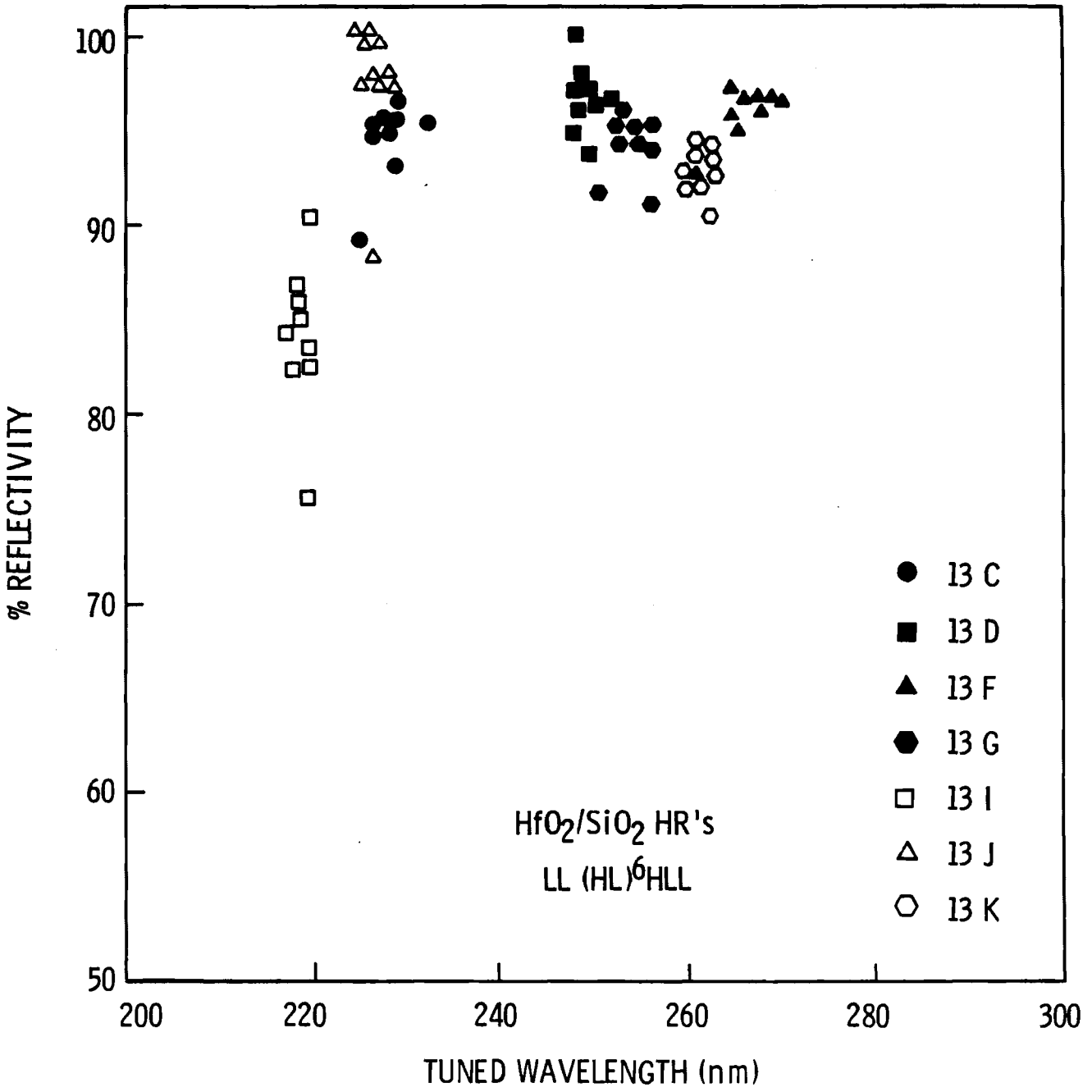

Figure 8. Variation of reflectivity of HfO_2/SiO_2 mirrors with tuned wavelength.

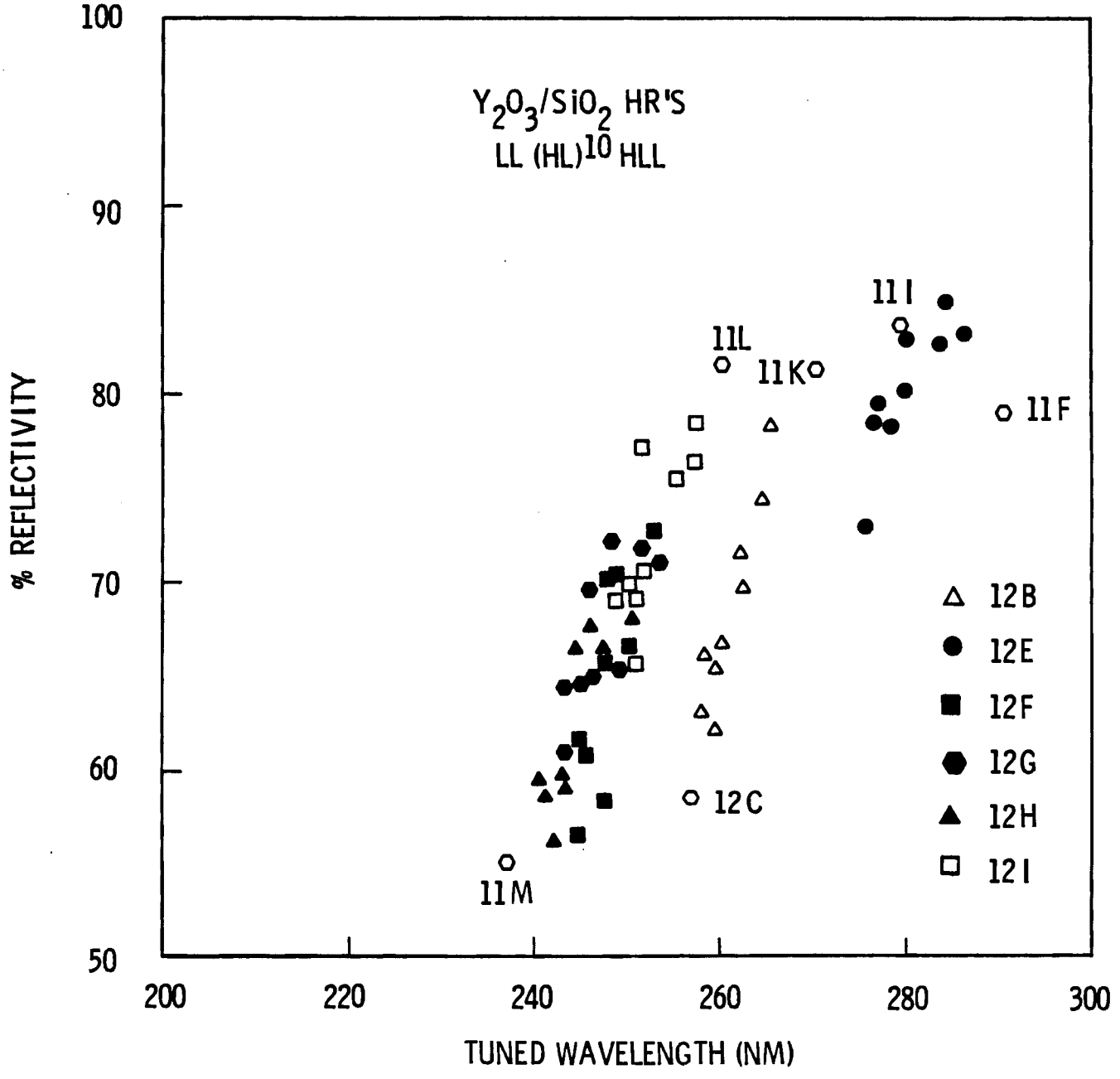

Figure 9. Variation of reflectivity of Y_2O_3/SiO_2 mirrors with tuned wavelength.

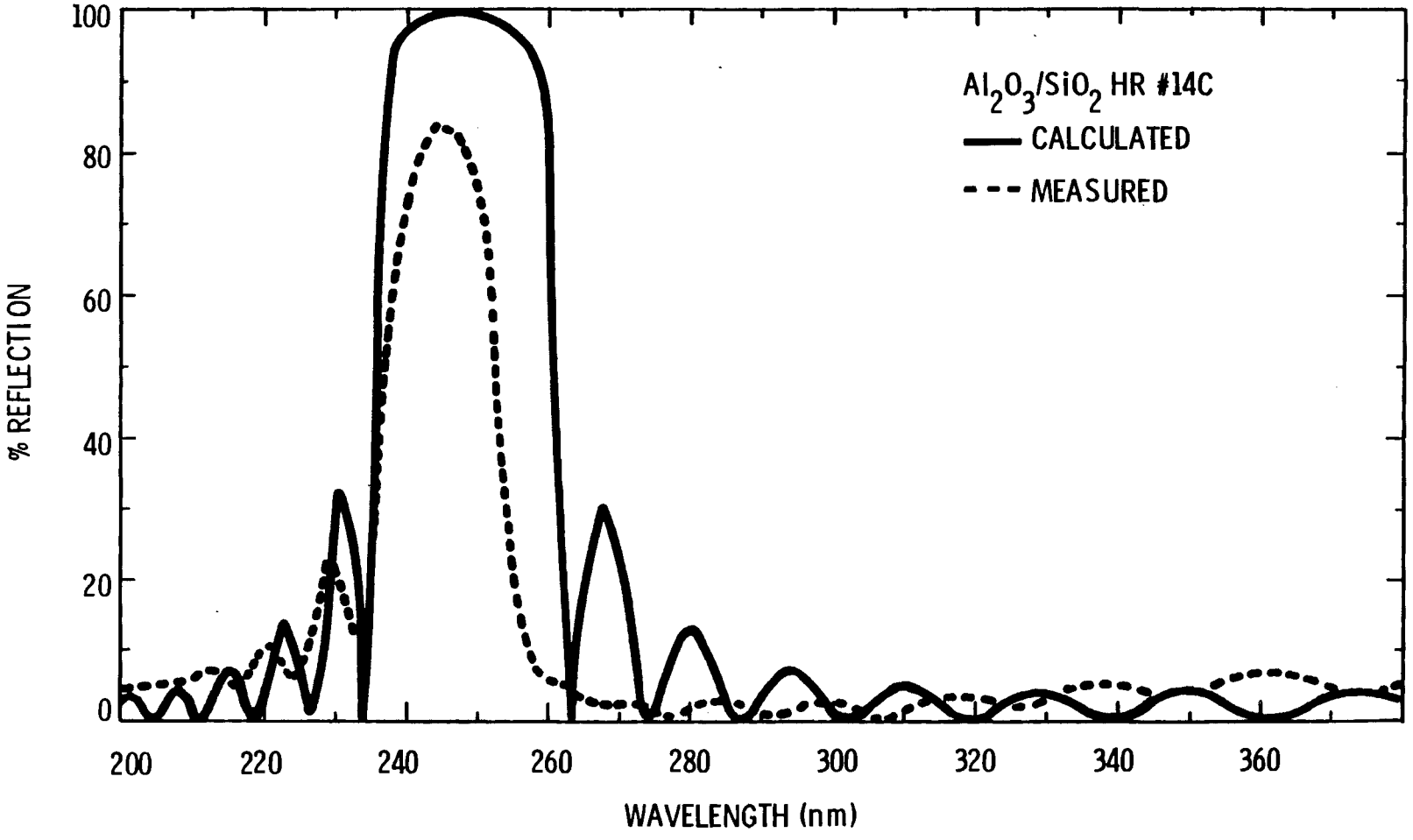

Figure 10. Spectral dependence of the reflectivity for an Al_2O_3/SiO_2 high reflector.

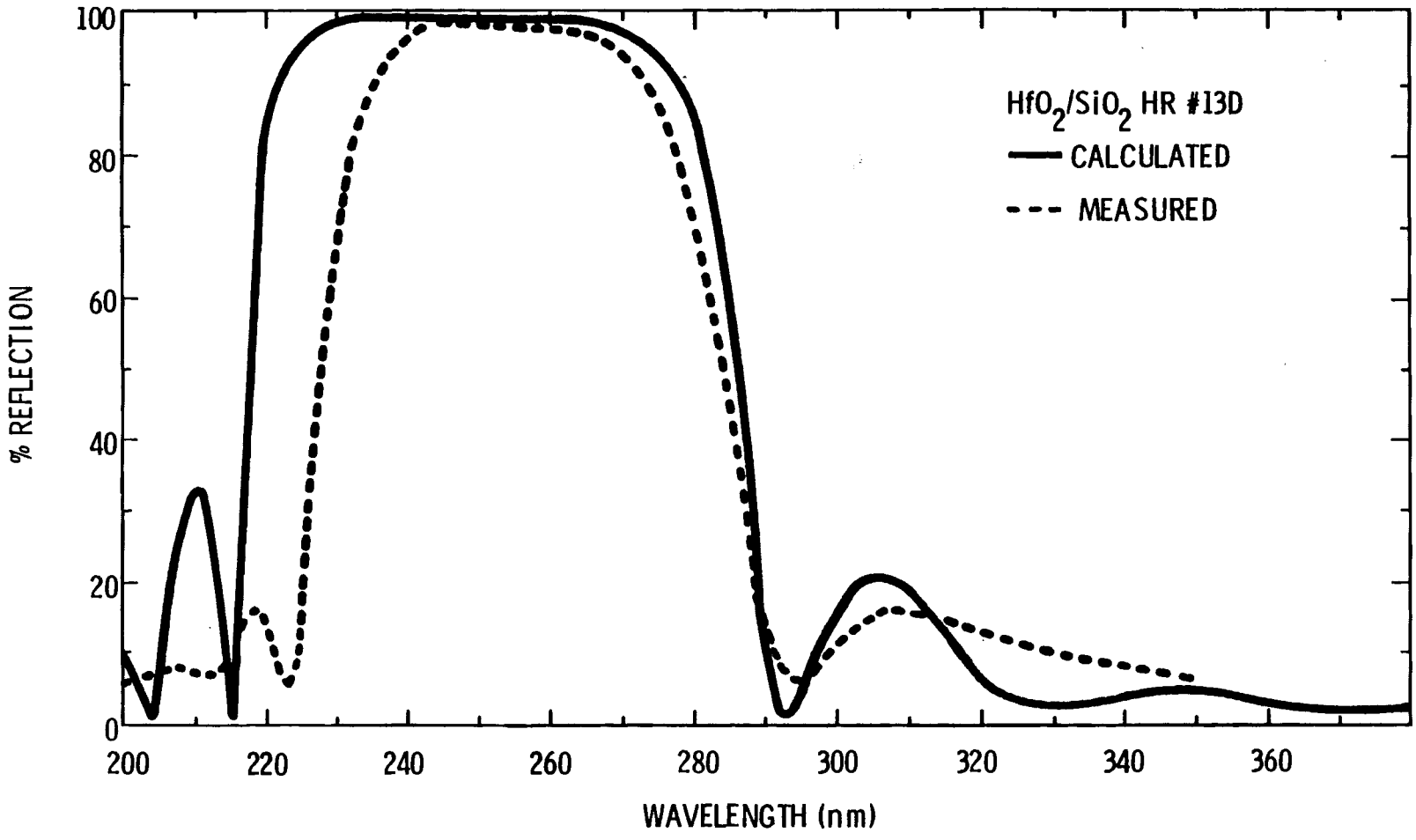

Figure 11. Spectral dependence of the reflectivity for a HfO_2/SiO_2 high reflector.

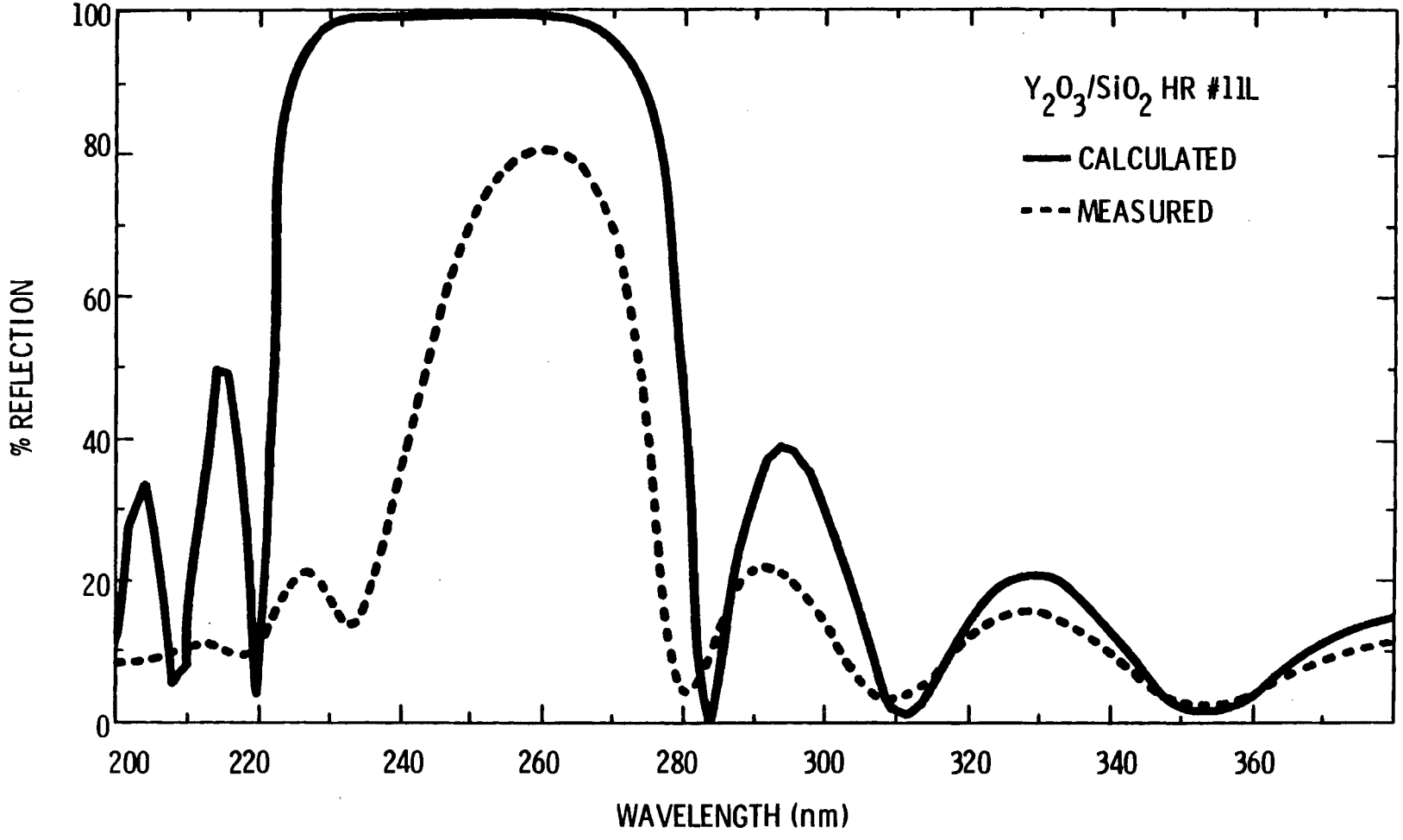

Figure 12. Spectral dependence of the reflectivity for an Y_2O_3/SiO_2 high reflector.

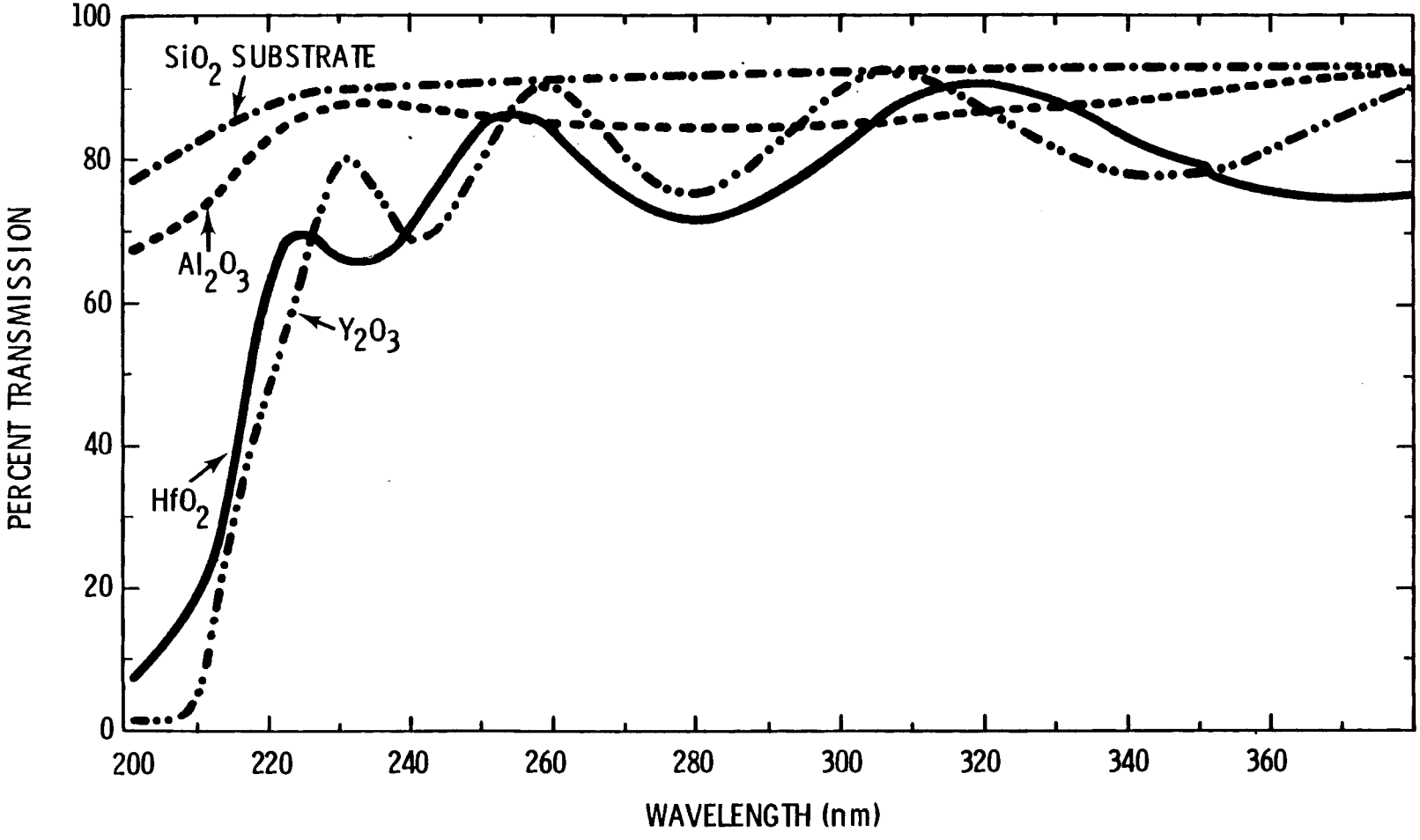

Figure 13. Transmission spectra for single layers of HfO_2, Y_2O_3 and Al_2O_3 on fused silica substrates.

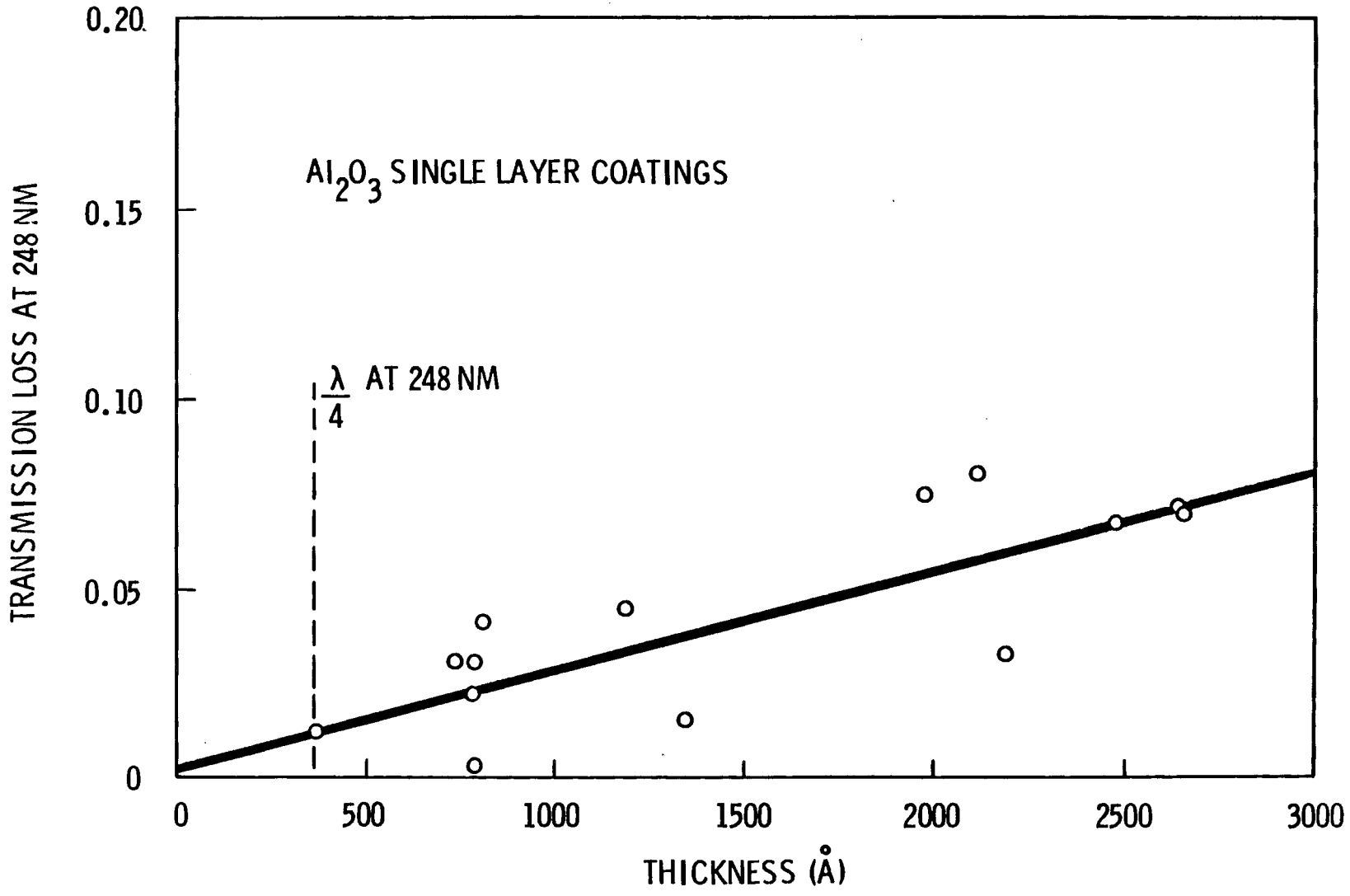

Figure 14. Dependence of Al_2O_3 scattering/absorption loss at 248 nm on single-layer coating thickness.

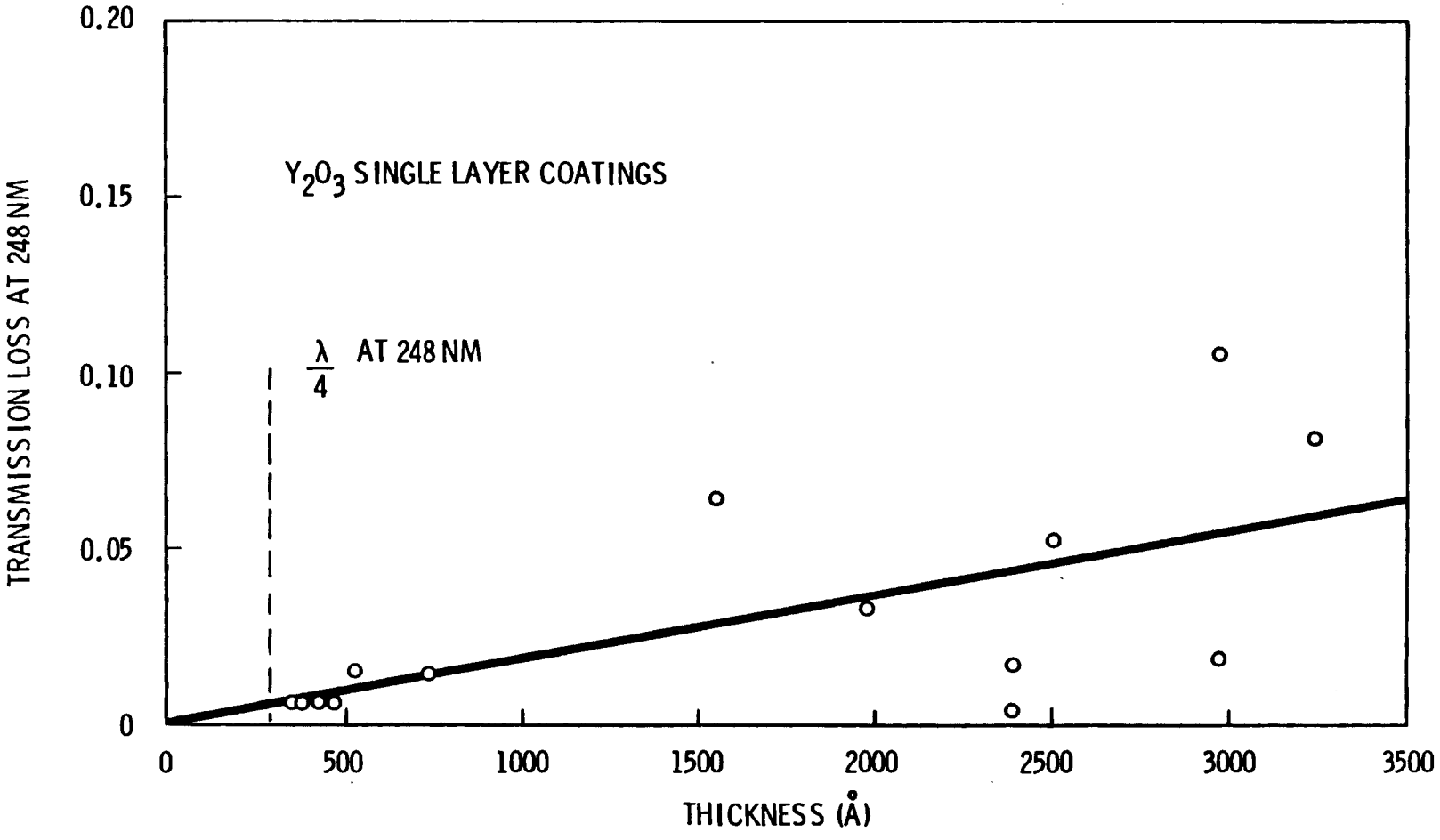

Figure 15. Dependence of Y_2O_3 scattering/absorption loss at 248 nm on single-layer coating thickness.

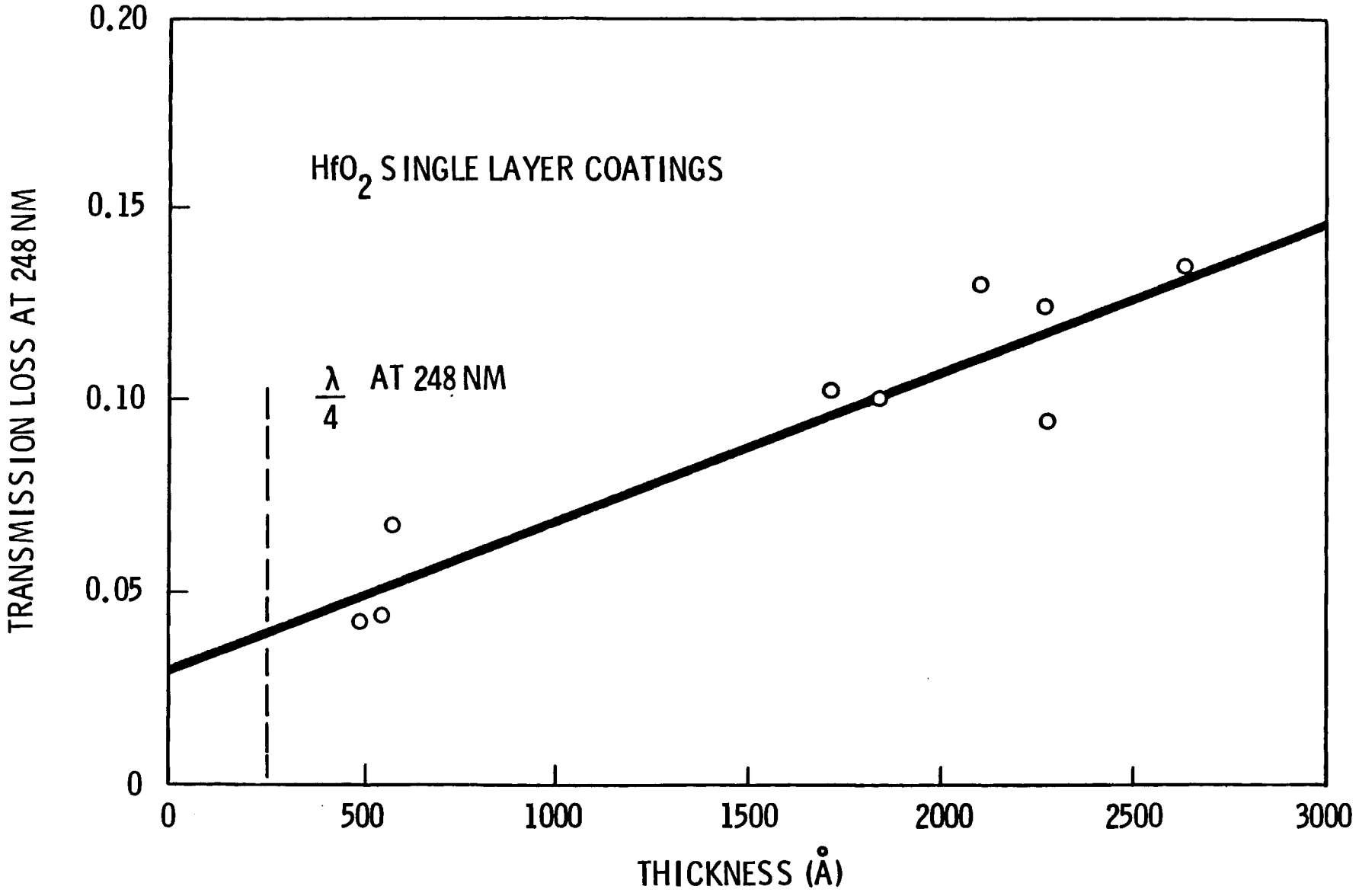

Figure 16. Dependence of HfO_2 scattering/absorption loss at 248 nm on single-layer coating thickness.[2]

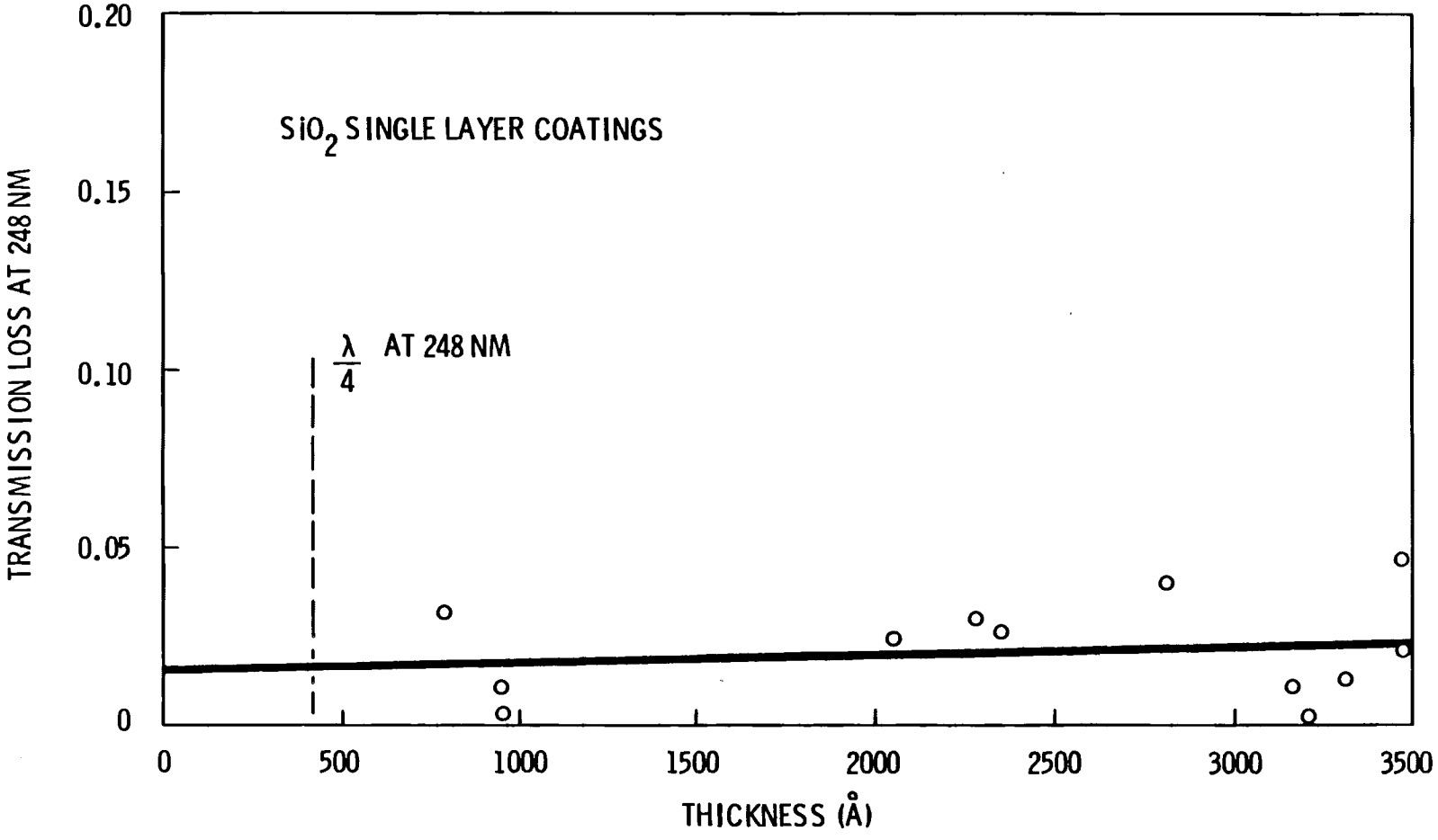

Figure 17. Dependence of SiO_2 scattering/absorption loss at 248 nm on single-layer coating thickness.[2]

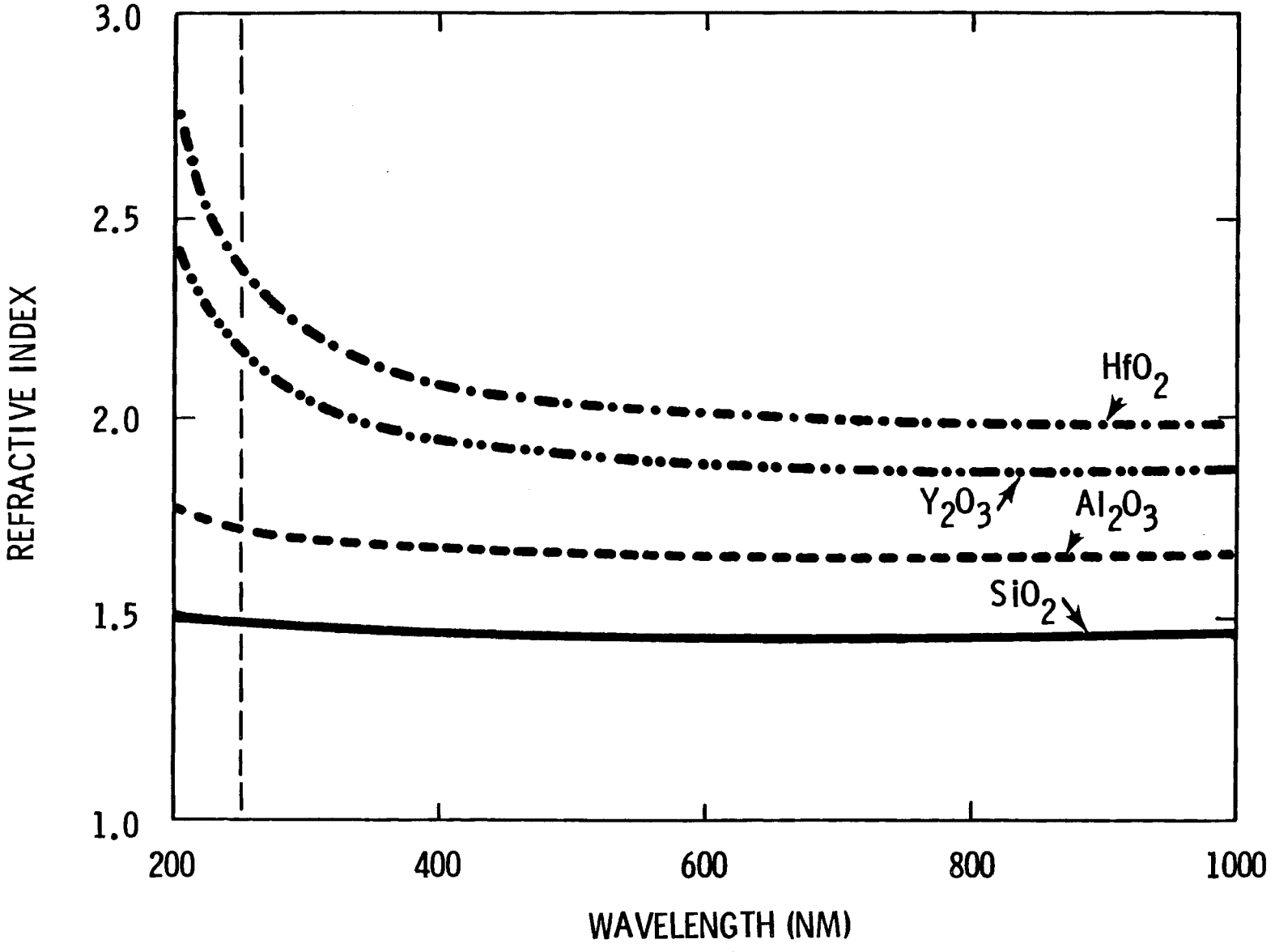

Figure 18. Refractive index variation with wavelength for HfO_2, Y_2O_3.Al_2O_3 and SiO_2.

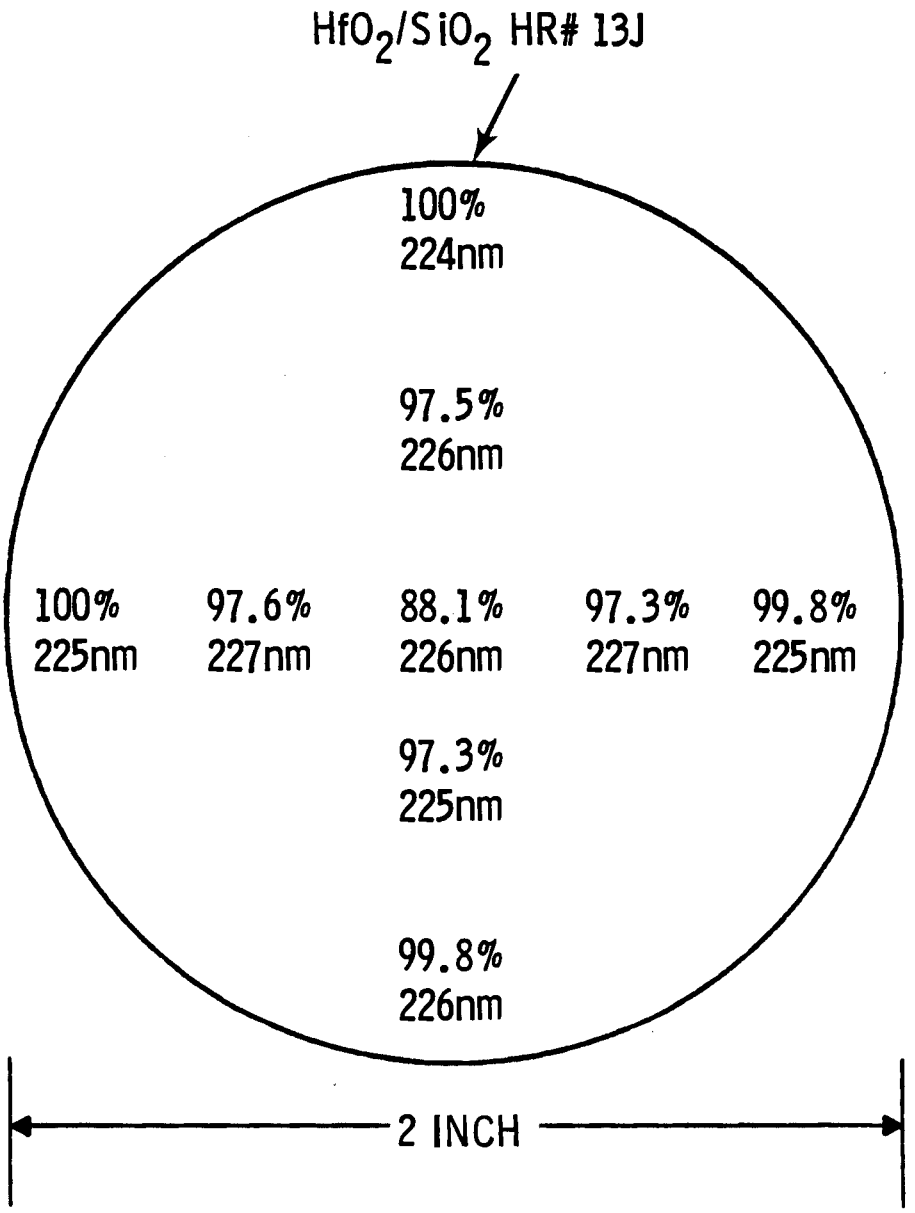

Figure 19. Reflectivity and tuned wavelength profile for a typical two-inch diameter HfO_2/SiO_2 mirror. Note the radial dependence of the reflectivity.

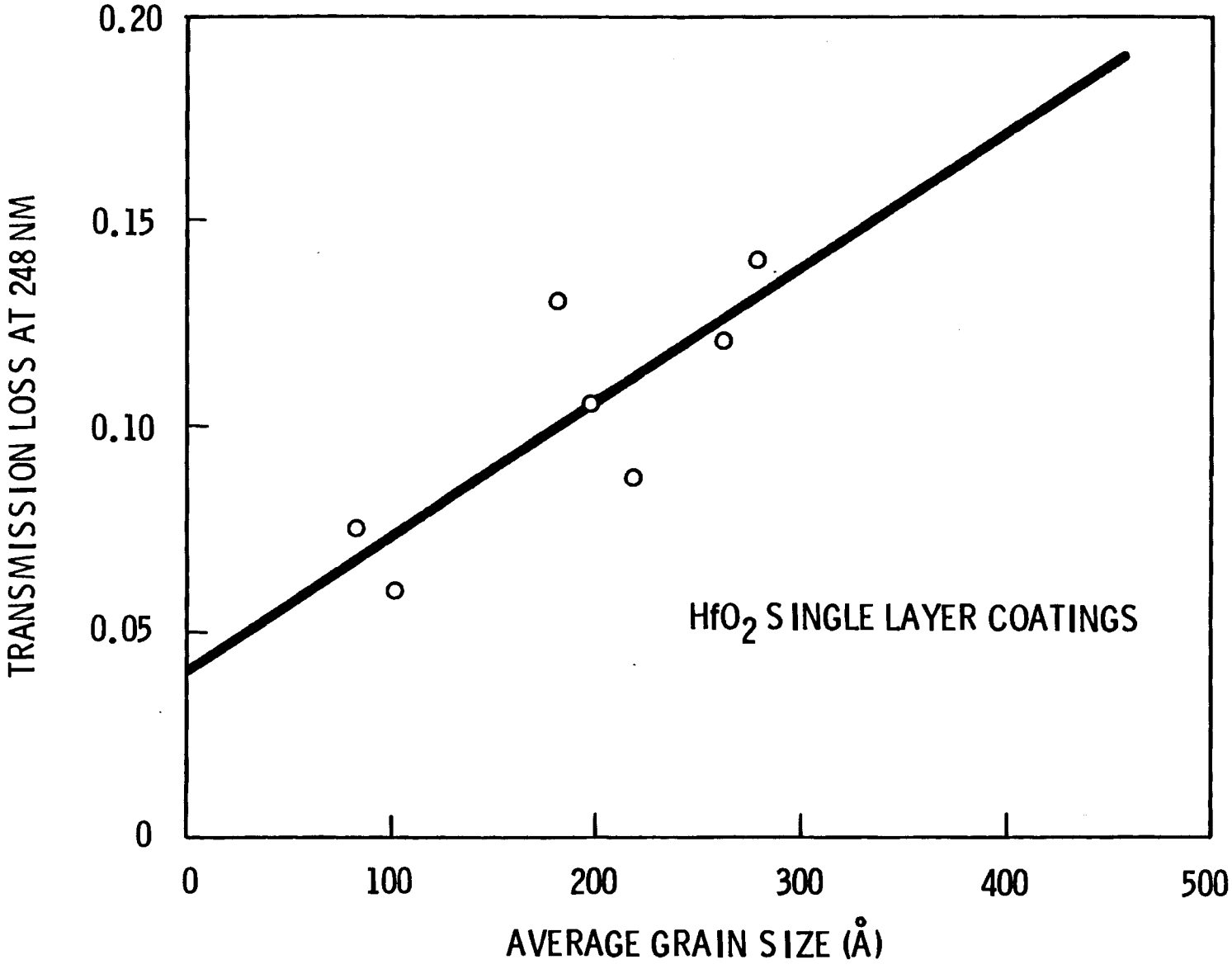

Figure 20. Influence of grain size on transmission loss due to scattering at 248 nm for approximately constant coating thickness of 2500 Å.

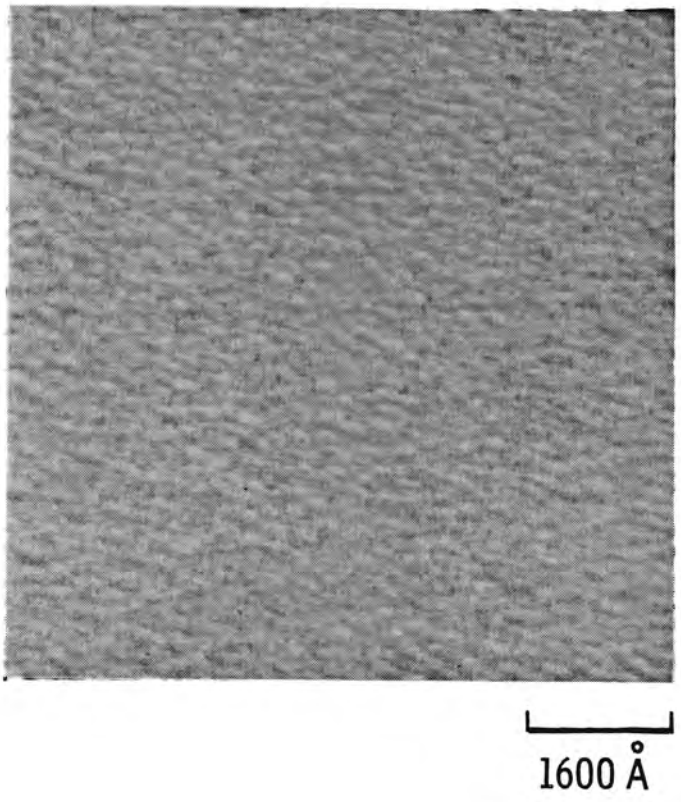

Figure 21. SEM micrograph of the surface topography of a 23-layer Y_2O_3/SiO_2 mirror.

APPENDIX

OXIDE OPTICAL COATINGS FOR THE ULTRAVIOLET

OXIDE OPTICAL COATINGS FOR THE ULTRAVIOLET

Compiled from the literature by W.T. Pawlewicz
Pacific Northwest Laboratory
May, 1980

SUMMARY

The recent literature is reviewed to compile a list of candidate oxide optical coating materials for use in high power ultraviolet (UV) lasers operating near 250 nm wavelength. The list includes representative absorption edge and refractive index values for both bulk and thin film oxides, as well as other potentially important properties of the materials such as hygroscopicity, toxicity, radioactivity, cost, etc. Eleven simple oxides which transmit at $\lesssim$ 250 nm are identified as prime candidates. The prime candidates are the common oxides of Si, Al, Be, Mg, Zr, Hf, Sc, Y, La, Nd and Th, which cover a range of refractive indices from 1.5 to 2.5 near 250 nm. The absorption edge values reported for coatings are found to lie at longer wavelengths than those reported for bulk materials. The difference apparently results from impurities, stoichiometric deviations and scattering in the coatings, and suggests that improvements in state-of-the-art coating technology will be necessary to realize the absorption edge values for bulk materials. A scarcity of data for wavelengths below 200 nm is also noticeable in the compilation for coatings, making it difficult to discern the absorption edges presently attainable. The oxides of Ca, Sr, Ba, Pr, Sm, Gd, B, Ga, Ge and Li are also listed as candidates because they transmit in the UV. However, very little optical coating research has been done to date with these materials and more study is required to assess there usefulness for UV applications. A final group of oxides deserving serious consideration is the mixed oxides consisting of two or more simple oxides combined in the appropriate proportions to form intermediate compounds, solid solutions and insoluble systems. Candidate oxides in this class are too numerous to list, but include materials such as $MgAl_2O_4$ ($MgO \cdot Al_2O_3$) and $Y_4Al_2O_9$ ($2Y_2O_3 \cdot Al_2O_3$). These mixed oxides generally exhibit absorption edges and refractive index values nearly identical to their constituent simple oxides, but may not exhibit undesirable physical properties of the constituent simple oxides such as hygroscopicity, color centers near 250 nm, etc.

OXIDE OPTICAL COATING MATERIALS FOR THE ULTRAVIOLET

Data Obtained from the Literature by
W.T. Pawlewicz (5-80)

Material	Absorption Edge (nm)	UV Index	VIS Index	IR Index	Reference	Comments (Ref.)
		SIMPLE OXIDE PRIME CANDIDATES				
SiO_2 (glass)	< 200	1.51 @ 250	1.50 @ 550	1.50 @ 1000	1	
	160b				2	
	< 200	1.52 @ 266	1.51 @ 355		3	
		1.58 @ 200	1.46 @ 500	1.44 @ 2000	7	
	155b				6	
	159b	1.49 @ 300b			16	
	144-153b	1.51 @ 249b	1.48 @ 354b		15	
Al_2O_3	< 200	1.75 @ 250	1.68 @ 550	1.67 @ 1000	1	
	130b				2	
	< 200	1.67 @ 266	1.65 @ 355		3	
		1.7 @ 200	1.63 @ 500	1.6 @ 2000	7	
	145b				6	
	141-149b	1.84 @ 2.49	1.79 @ 354		15	
	141b	1.8 @ 300			16	
ZrO_2	240	2.47 @ 250	2.18 @ 550	2.15 @ 1000	1	
	260	2.4 @ 266	2.27 @ 355		3	(Sputtered)
	225	2.17 @ 266	1.95 @ 355		3	(Evaporated)
			2.1 @ 500	2.0 @ 2000	7	
	235				6	
	270	2.1 @ 300			16	
	240	2.1 @ 300			17	

b = bulk material value

Material	Absorption Edge (nm)	UV Index	VIS Index	IR Index	Reference	Comments (Ref.)
			SIMPLE OXIDE PRIME CANDIDATES			
HfO_2	220	2.15 @ 266	2.08 @ 355		3	
	230				6	
		2.12 @ 250	1.98 @ 500	1.95 @ 1000	14	(After bake)
		2.31 @ 250	2.05 @ 500	1.97 @ 1000	14	(Before bake)
	240		2.14 @ 350		16	
	225	2.1 @ 300			17	
Y_2O_3	215	2.0 @ 266	1.79 @ 355		3	Hygroscopic starting materials (4)
			1.88 @ 500		4	(Thin Films)
			2.06 @ 500		4	(Thick Films)
		1.88 @ 250	1.78 @ 500	1.75 @ 1000	14	(After bake)
		1.98 @ 250	1.82 @ 500	1.78 @ 1000	14	(Before bake)
	~ 200				16	
La_2O_3	220	2.16 @ 250	1.96 @ 550	1.93 @ 1000	6	Low packing density (6)
			1.85 @ 500		4	(Thin Films, 300°C)
						Hygroscopic starting materials (4)
			2.16 @ 500		4	(Thick Films, 20°C)
						Low packing density (4)
	210				6	
		1.92 @ 250	1.86 @ 500	1.84 @ 1000	14	(After bake)
		2.10 @ 250	1.89 @ 500	1.83 @ 1000	14	(Before bake)
Sc_2O_3	~ 200	1.9-2.0@250				Expensive
	210				15	

b = bulk material value

Material	Absorption Edge (nm)	UV Index	VIS Index	IR Index	Reference	Comments (Ref.)
			SIMPLE OXIDE PRIME CANDIDATES			
BeO	120b				2	Toxic
	200	1.76 @ 250	1.69 @ 514	1.68 @ 1000	6	
			1.68 @ 500		5	
	195				6	
	124b				16	
			1.73 @ 589b		11	
MgO	160b				2	Hygroscopic
	210				6	
			1.736@ 589b		11	
	175b	1.74 @ 250b			16	
	< 200	1.74 @ 250			15	
ThO_2	250	2.0 @ 266	1.95 @ 355		3	Slightly radioactive (14)
		1.9 @ 300	1.8 @ 500	1.75 @ 2000	7	Extremely refractory - difficult to evaporate (14)
	260				6	
	214b	1.95 @ 300			16	
Nd_2O_3	255	2.02 @ 250	1.87 @ 550	1.85 @ 1000	6	Low packing density (6)
			2.05 @ 500		4	Hygroscopic starting materials (4)
	250				6	

b = bulk material value

Material	Absorption Edge (nm)	UV Index	VIS Index	IR Index	Reference	Comments (Ref.)
			CANDIDATES, BUT REQUIRE MORE STUDY			
CaO	160b				2	Soluble: 0.13g/100g H_2O @ 20°C (11)
			1.84 @ 589		11	
SrO	~ 200				13	Soluble: 0.69g/100g H_2O @ 20°C (11)
			1.81 @ 589		11	
BaO	~ 260				13	Soluble: 3.48g/100g H_2O @ 20°C (11)
			1.98 @ 589		11	
Pr_6O_{11}	$\lesssim$ 300		1.92-2.05 @ 500		4	Hygroscopic starting materials (4)
Sm_2O_3			2.05-2.2 @ 500		4	Hygroscopic starting materials (4) Deposition uncontrolled (4) Absorptive (4)
Gd_2O_3			2.05-2.2 @ 500		4	Hygroscopic starting materials (4) Deposition uncontrolled (4) Absorptive (4)
GeO_2 (hex)			1.65 @ 589b		11	Soluble: 0.447g/100g H_2O @ 20°C (11)
GeO_2 (tetr.)						Insoluble (11)

b = bulk material value

Material	Absorption Edge (nm)	UV Index	VIS Index	IR Index	Reference	Comments (Ref.)
			CANDIDATES, BUT REQUIRE MORE STUDY			
GeO			1.60 @ 589b		11	Sublimes @ 710°C (11)
B_2O_3 (rhomb.)			1.63 @ 589b		11	Slightly soluble in H_2O (11) M.P. = 460°C (11)
B_2O_3 (vitreous)			1.485@ 589b		11	Soluble: 1.1g/100g H_2O @ 20°C (11) M.P. = 450°C (11)
Li_2O			1.644@ 589b		11	Soluble: 6.67g/100g H_2O @ 20°C (11)
Ga_2O_3	~ 280		1.93 @ 589b		13	
			MIXED OXIDE PRIME CANDIDATES			
$MgAl_2O_4$ ($MgO \cdot Al_2O_3$)	225	1.90 @ 250	1.64 @ 500	1.61 @ 1000	1	
$Y_4Al_2O_9$ ($(2)Y_2O_3 \cdot Al_2O_3$)	220	1.97 @ 250	1.78 @ 500	1.76 @ 1000	1	

b = bulk material value

Material	Absorption Edge (nm)	UV Index	VIS Index	IR Index	Reference	Comments (Ref.)
		MIXED OXIDE PRIME CANDIDATES				
$CaCO_3$ (calcite)	240b	1.90) 1.58) @ 200	(birefringent)	1.62) 1.47) @ 2500	10,12	
	$\lesssim$ 200				13	
$BeAl_2O_4$ ($BeO \cdot Al_2O_3$)		1.75 @ 589			11	

+ Numerous unexplored compound-forming systems, solid solutions and insoluble systems formed from the simple oxides listed above.

b = bulk material value

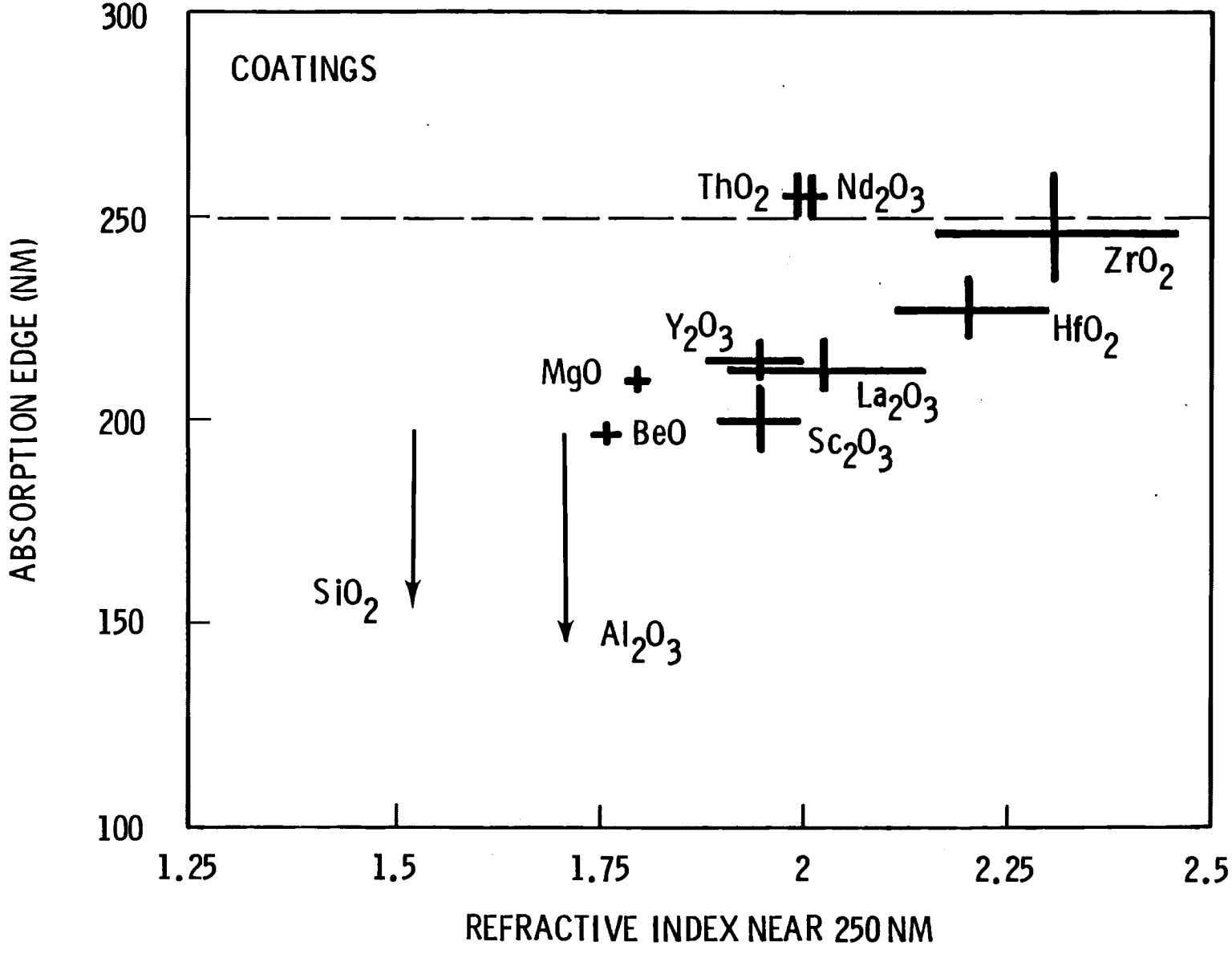
COATINGS
ThO2
Nd2O3
ZrO2
HfO2
Y2O3
MgO
BeO
La2O3
Sc2O3
SiO2
Al2O3
300
250
200
150
100
1.25
1.5
1.75
2
2.25
2.5
ABSORPTION EDGE (NM)
REFRACTIVE INDEX NEAR 250 NM

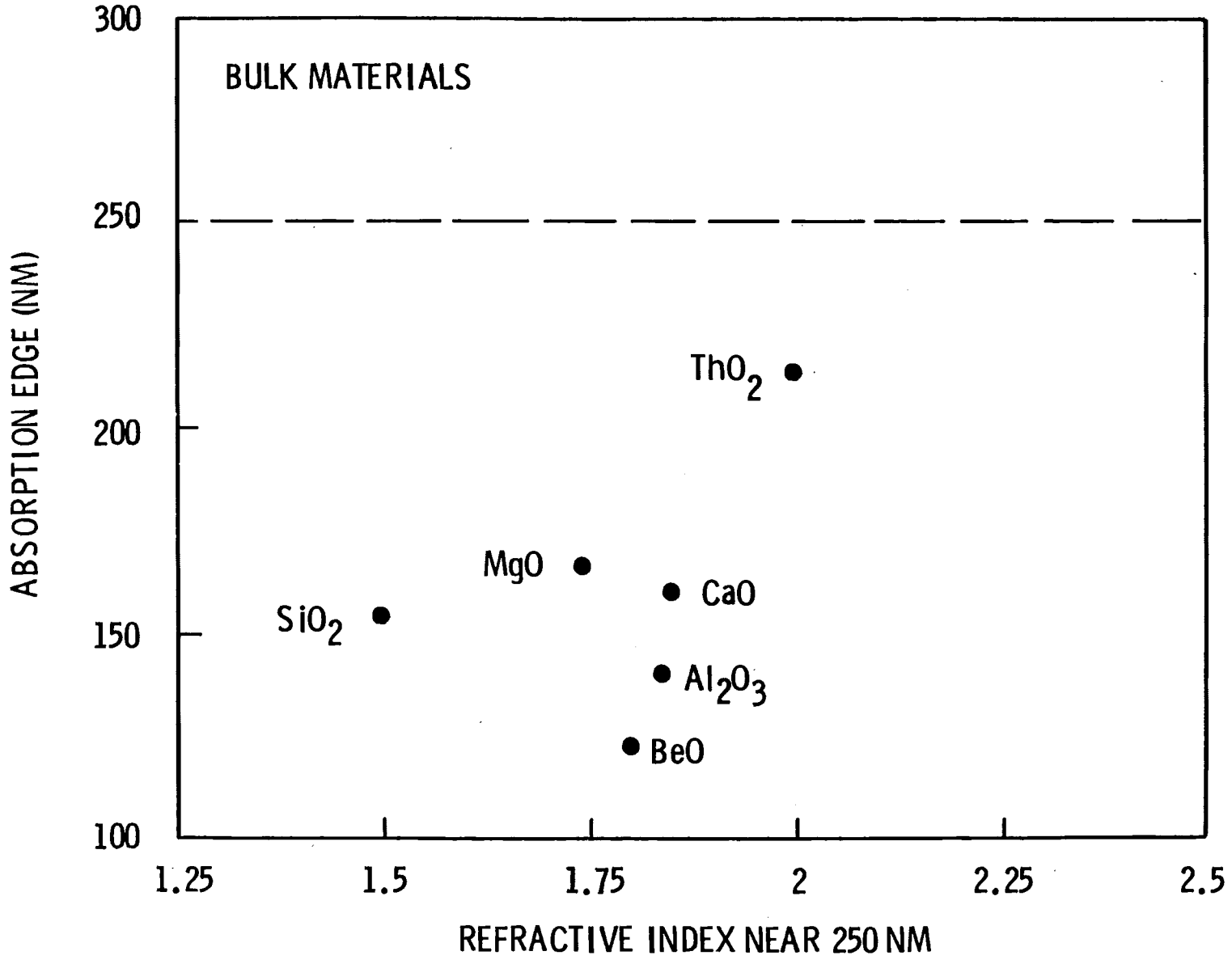
BULK MATERIALS
ABSORPTION EDGE (NM)
300
250
200
150
100
ThO2
MgO
CaO
SiO2
Al2O3
BeO
1.25
1.5
1.75
2
2.25
2.5
REFRACTIVE INDEX NEAR 250 NM

REFERENCES FOR APPENDIX

1. W.T. Pawlewicz, D.D. Hays and P.M. Martin, "High-Band-Gap Oxides for 0.25 and 1.06 μm Fusion Lasers", Thin Solid Films 73 (1980) 169-175.

2. A. Feldman, R.M. Waxler and I.H. Malitson, "Survey of Refractive Data on Materials for High-Power Ultraviolet Laser Applications", in Proceedings of the Society of Photo-Optical Instrumentation Engineers, Vol. 204, Physical Properties of Optical Materials, pp. 95-101.

3. B.E. Newnam and D.H. Gill, "Ultraviolet Damage Resistance of Laser Coatings", in Laser Induced Damage in Optical Materials: 1978 (NBS Spec. Pub. 541), Edited by A.J. Glass and A.H. Guenther, pp. 190-201.

4. G. Hass, J.B. Ramsey and R. Thun, "Optical Properties of Various Evaporated Rare Earth Oxides and Fluorides", J. Opt. Soc. Amer. 49 (2), (1959) 116-120.

5. H. Gruner, "Einege lichtoptische Eigenschaften reaktiv aufgedampfter Berylliumoxid-Schichten", Optik 39 (4), (1974) 443-449.

6. H. Küster and J. Ebert, "Pyroelectric Measurement of Absorption in Oxide Layers and Correlation to Damage Threshold", in Laser Induced Damage in Optical Materials: 1979 (NBS Spec. Pub., 568), Edited by A.J. Glass, A.H. Guenther, H. Bennett and B. Newnam, pp. 269-279.

7. G. Hass and E. Ritter, "Optical Film Materials and Their Applications", J. Vacuum Science and Technology 4 (2), (1967).

8. Electronic, Optical and Laser Materials and Components, Adolf Meller Co., Providence, RI.

9. Handbook of Tables for Applied Engineering Science, The Chemical Rubber Co., p. 220.

10. Harshaw Optical Crystals, The Harshaw Chemical Company.

11. Handbook of Chemistry and Physics, The Chemical Rubber Co.

12. Handbook of Optics of the Optical Society of America, W.G. Driscoll and W. Vaughan, eds., (McGraw-Hill, 1978).

13. American Institute of Physics Handbook, D.E. Gray, ed. (McGraw-Hill, 1972).

14. P. Baumeister, "Optical Interference Coatings for the Ultraviolet", Final Progress Report to Office of Naval Research, Contract N00014-77-C-0573, (Aug. 1, 1977 to July 31, 1978).

15. H.E. Bennett, A.D. Baer, R.S. Hughes, V. Rehn and J.L. Stanford, "Ultraviolet Components for High Energy Applications", First Annual Report to DARPA (NWC TP 6015) March 1978.

16. M. Sparks and C.J. Duthler, "Theoretical Studies of High-Power Ultraviolet and Infrared Materials", 8th Technical Report, December 1976, DARPA Contract No. DAHC 15-73-C-0127. (Xonics, Inc., Santa Monica, CA, 1976).

17. P. Baumeister, Appl. Opt. 15 (1976) 2313.

DISTRIBUTION

No. of Copies

OFFSITE

A. A. Churm
DOE Patent Division
9800 South Cass Avenue
Argonne, Illinois 60439

20 W. Howard Lowdermilk
Lawrence Livermore National Lab.
Mailstop L-465
P.O. Box 5508
Livermore, CA 94550

27 DOE Technical Information Center

David Milam
Lawrence Livermore National Lab.
Mailstop L-465
P.O. Box 5508
Livermore, CA 94550

Frank Rainer
Lawrence Livermore National Lab.
Mailstop L-465
P.O. Box 5508
Livermore, CA 94550

No. of Copies

ONSITE

DOE Richland Operations Office

H. E. Ransom

31 Pacific Northwest Laboratory

Walter T. Pawlewicz (20)
Darrell D. Hays
Peter M. Martin
Ira B. Mann
James W. Patten
Publishing Coordination (2)
Technical Information (5)